plasma

Review

A Comprehensive Review on Amplification of Laser Pulses via Stimulated Raman Scattering and Stimulated Brillouin Scattering in Plasmas

Renju Miriam Cheriyan [1], Nikhil Varghese [1], R. S. Sooraj [1], Kavya H. Rao [2,*] and N. Smijesh [1,2,*]

[1] Ultrafast Optics Group, School of Pure and Applied Physics, Mahatma Gandhi University, Priyadarsini Hills P. O., Kottayam 686560, India
[2] ELI Beamlines Centre, Institute of Physics AS ČR, Za Radnici 835, 252 41 Dolní Břežany, Czech Republic
* Correspondence: kavya.rao@eli-beams.eu (K.H.R.); smijeshn@mgu.ac.in (N.S.)

Abstract: The demand for high-intensity lasers has grown ever since the invention of lasers in 1960, owing to their applications in the fields of inertial confinement fusion, plasma-based relativistic particle accelerators, complex X-ray and gamma-ray sources, and laboratory astrophysics. To create such high-intensity lasers, free-running lasers were either Q-switched or mode-locked to increase the peak power to the gigawatt range. Later, chirped pulse amplification was developed, allowing the generation of peak power up to 10^{12} W. However, the next generation of high-intensity lasers might not be able to be driven by the solid-state technology alone as they are already operating close to their damage thresholds. In this scenario, concepts of amplification based on plasmas has the potential to revolutionize the laser industry, as plasma is already a broken-down medium, and hence does not pose any problems related to the damage thresholds. On the other hand, there are many other aspects that need to be addressed before developing technologies based on plasma-based amplification, and they are being investigated via theoretical and numerical methods and supported by several experiments. In this report, we review the prospects of employing plasma as the medium of amplification by utilising stimulated scattering techniques, such as the stimulated Raman scattering (SRS) and stimulated Brillouin scattering (SBS) techniques, to modulate high-power laser pulses, which would possibly be the key to the next generation of high-power lasers. The 1980s saw the commencement of research in this field, and possibilities of obtaining high peak powers were verified theoretically with the help of numerical calculations and simulations. The extent of amplification by these stimulated scattering schemes are limited by a number of instabilities such as forward Raman scattering (FRS), filamentation, etc., and here, magnetised plasma played an important role in counteracting these parasitic effects. The current research combines all these factors to experimentally realise a large-scale plasma-based amplifier, which can impact the high-energy laser industry in the near future.

Keywords: amplification; plasma; high-power lasers; chirped pulse amplification; parametric processes; stimulated Raman scattering (SRS); stimulated Brillouin scattering (SBS); magnetised plasma

Citation: Miriam Cheriyan, R.; Varghese, N.; Sooraj, R.S.; Rao, K.H.; Smijesh, N. A Comprehensive Review on Amplification of Laser Pulses via Stimulated Raman Scattering and Stimulated Brillouin Scattering in Plasmas. *Plasma* **2022**, *5*, 499–539. https://doi.org/10.3390/plasma5040037

Academic Editor: Andrey Starikovskiy

Received: 11 September 2022
Accepted: 17 November 2022
Published: 24 November 2022

1. Introduction

The demand for high-intensity lasers has increased ever since the development of lasers in 1960 [1], owing to the applications of lasers, ranging from the principles governing optical ionisation processes of individual atoms to the collective reactions of laser-driven plasmas [2,3], such as inertial confinement fusion [4–9], plasma-based relativistic particle accelerators [10–16], complicated X-ray [17–20] and gamma-ray sources [21,22], or laboratory astrophysics [23–25]. In order to produce gigawatt-level (10^9 W) peak power in picosecond (ps) pulses, free-running laser oscillators were Q-switched and/or mode-locked in the 1960s [26]. Later, arrays of laser amplifiers further increased the peak power of gigawatt pulses [27,28]. However, beyond this power, the refractive index of the material varies nonlinearly and distorts the laser pulses [29]. Therefore, practically no advancements were made in the field of laser pulse amplification for almost 20 years until the technique of chirped pulse amplification (CPA) [30] was introduced in 1980. The majority of the high-power laser systems developed after the 1980s utilized the CPA technique to deliver high peak powers (10^6–10^{12} W) at short pulse durations (5–100 femtoseconds (fs)), capable of producing intensities of the order of 10^{22} W/cm^2 [31,32]. However, the laser crystal and the stretcher/compressor gratings are crucial components of CPA-based amplifier, which can be easily damaged when operating near their respective damage threshold [33]. Hence, the only method by which to further amplify the laser pulse is the upgrading of crystals and compressors, e.g., through the use of two parallel diffraction gratings [29]. To attain power of the order of petawatt (10^{15} W, PW), grating of $\sim$1 m diameter are required [34], which means that hundreds of such gratings would be required to extend the available power to the exawatt (10^{18} W) range [29], making the development of such a system extremely costly and time-consuming, with the major drawback that they are easily harmed by the intensity of light [35]. A timeline of these developments is given in Figure 1.

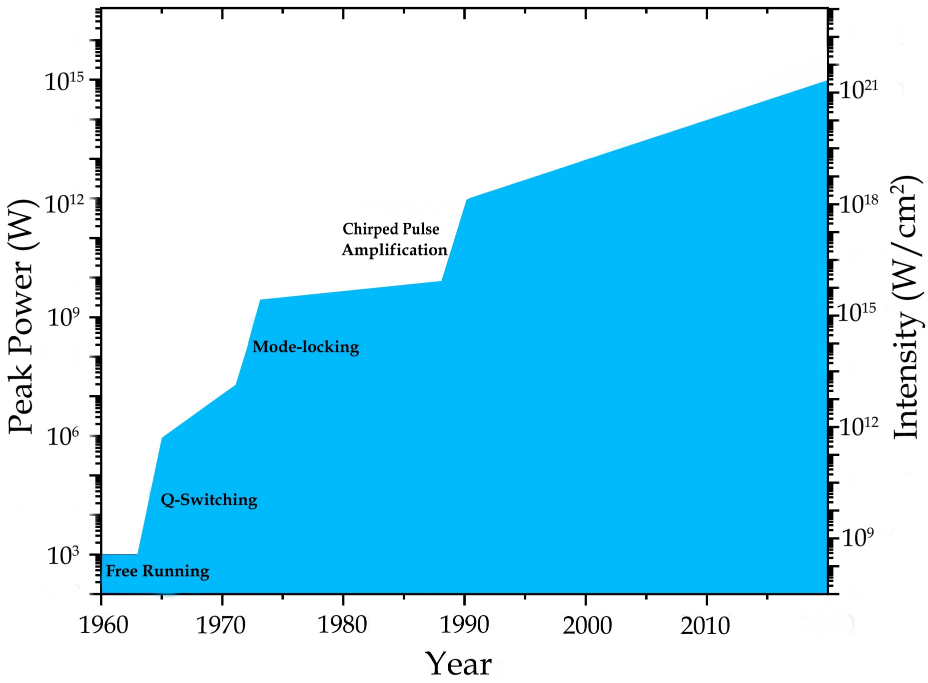

Figure 1. Pulsed laser peak power has increased over the past years as a result of introduction of succession of new techniques. The intensity available at the focal spot of the laser beam is presented on the right-Y axis.

The use of gases, liquids, and plasmas as amplifying media provides solutions that go beyond the limitations of solid optical materials [36–38] and achieve higher laser powers. Although the damage limits for compression systems based on reverse parametric amplification in liquids or gases are substantially greater, the pulse length in such systems is constrained by the phonon period, which is of the order of 100 picoseconds (ps) [39]. Therefore, suggestions to employ plasma as an amplifying medium were introduced, owing to their significantly greater damage thresholds [40–42], as they are already ionised matter, and various processes occurring in plasma supports amplification. In addition to serving as an amplifying medium, plasma can also be utilised to manipulate extremely powerful laser pulses [43–46]. The use of spatially structured plasmas as optical devices is another emerging area of research for the development of plasma-based optics [47,48], by which structured plasmas can be employed as polarizers or Bragg-type mirrors for ultrashort and powerful laser pulses [49]. Even though the area of research in which plasmas are employed for various applications in laser physics is growing fast and has a rich developmental history, the current review is based on the amplification of laser pulses in plasmas, especially via Raman and Brillouin processes in the plasma.

The three-wave energy coupling between a short seed pulse (tens to hundreds of fs) and a relatively longer and stronger pump pulse (of the order of ps or longer) forms the basis for plasma-based amplification and compression techniques. Both laser pulses generally have distinct frequencies and the objective of a plasma-based amplifier is to transfer the maximum possible energy to a short seed laser pulse that travels through plasma, in which an energetic counter-propagating pump pulse serves as the energy source. Collisions between particles are ignored in the most basic description of a plasma, and the particles only interact with one another through averaged magnetic and electrostatic fields produced by plasma currents and charge inhomogeneities. Therefore, a plasma can support two types of electrostatic waves in the absence of any externally applied strong magnetic fields: an electron plasma wave with a high frequency and an ion acoustic wave with a lower frequency, which are known as plasma waves. This plasma wave is used to mediate the energy transfer from the pump to the seed [35] as shown in Figure 2.

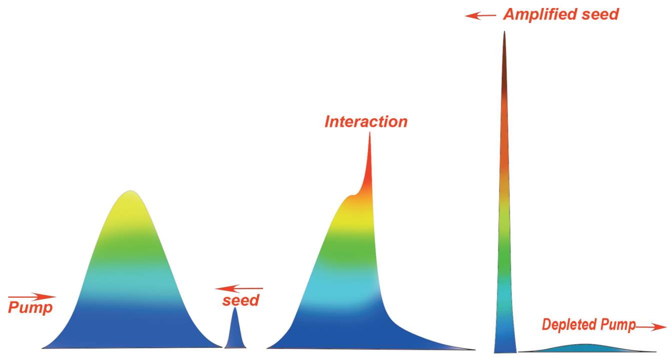

Figure 2. Schematic of laser amplification via stimulated Raman scattering and stimulated Brillouin scattering.

When the pulses cross each other, a beat is created at a frequency, $\omega_{plasma} = \omega_{pump} + \omega_{seed}$, where, ω_{plasma}, ω_{pump}, and ω_{seed} are the frequencies of plasma wave, pump, and the seed, respectively [35]. Resonant backscattering of the pump into the seed happens when the beat frequency is equal to the frequency of an undamped plasma oscillation, i.e., the seed pulse will be amplified at the expense of the pump. Once this process commences, the energy transfer continues even when the intensity of the seed is greater than that of the pump [35]. High-frequency electron Langmuir waves (SRS) or low-frequency ion waves (SBS) are the two possible plasma modes utilized for amplification [50]. Henceforth, the amplification due to SRS will be addressed as Raman amplification and the amplification due to SBS will be addressed as Brillouin amplification. The idea of amplifying laser pulses via instabilities in plasma (SRS and SBS) has been a topic of interest ever since they were identified to serve the purpose of barrier-free amplification [40–42,51,52]. However, it has only been explored widely in the recent years [52–63], complemented by an increase in efforts to use numerical simulations to optimise the parameters for strengthening these interactions [64–69]. In addition to this, the investigation of X-ray Raman amplification [70,71], the use of chirped laser pulses in Brillouin amplification and Raman amplification [69,72], and the investigation of a variety of unique pulse amplification configurations [73,74] has also drawn interest lately, allowing us to broaden the availability of potential amplifying media. The use of these amplification techniques in several fields of research has also contributed to its advancement. For example, at the National Ignition Facility in California, Brillouin scattering has also been employed to transmit energy via the cross-beam energy transfer scheme, allowing researchers to mitigate the adverse effects of the cross-beam energy transfer scheme [75–80]. Inertial confinement fusion [81–92], as well as wakefield acceleration [92–97] has been the subject of in-depth research on both Raman and Brillouin scattering.

Raman scattering and Brillouin scattering have various characteristics that can be utilized for laser beam amplification. For instance, the largest amplification ratios, E_{amp} (i.e., the ratio of output energy to input energy of the seed pulse) and shortest output pulses are produced by Raman amplification, but it is sensitive to changes in experimental parameters and demands a precise matching of the laser and plasma frequencies [98]. Lower peak intensities or amplification ratios are produced by Brillouin amplification, but it is resistant to parameter changes or frequency mismatches, more effective (as less laser energy is retained in the plasma wave), and better suited for the creation of pulses with a high total power or energy [98]. The current article evaluates the potential of SRS and SBS in the context of amplification of laser pulses because amplified laser pulses are widely used in various fields as mentioned earlier. To address the advantages and drawbacks of SRS and SBS, parameters specific to these processes are quantified in SI units, unless otherwise specified.

2. Stimulated Raman Scattering (SRS)

2.1. Theory

In amplification via SRS (also known as backward Raman amplification), energy is transferred from an electromagnetic wave of frequency ω_{pump} (pump) to another counter-propagating electromagnetic wave, which is at a lower frequency of ω_{seed} (seed), and the Langmuir wave having frequency ω_{plasma}. Therefore, it is referred to as a three-wave interaction process. The plasma medium is crucial here because, unlike other media supporting Raman processes such as gases or fibres, plasma is an ionised medium (i.e., considered as an "already broken-down" medium), and can endure extremely high intensities [99]. For the Raman interaction to take place, it is essential that the frequency and wavenumber matching conditions are represented mathematically as [100]

$$\omega_{pump} = \omega_{seed} + \omega_{plasma} \tag{1}$$

$$k_{plasma} = k_{pump} + k_{seed} \tag{2}$$

and are satisfied. Here, ω_{pump}, ω_{seed} and ω_{plasma} are the frequencies of the pump laser, seed laser, and the Langmuir wave, respectively. k_{pump}, k_{seed} and k_{plasma} are the wavenumbers of the pump laser, seed laser, and the Langmuir wave, respectively. These conditions ensure that the energy and momentum conservation is satisfied, i.e., it ensures that a driving force in resonance with the third wave is produced as a result of the nonlinear interaction of the other two waves [100]. In terms of the laser wavelength of the pump λ_{pump_0} and seed λ_{seed0} in vacuum, the expression for pump and seed laser frequencies can be written as [101]

$$\omega_{pump(seed)} = \frac{2\pi c}{\lambda_{pump0}(\lambda_{seed0})} \approx \frac{1.9 \times 10^{11}}{\lambda_{pump0}(\lambda_{seed0})/(cm)}\ sec^{-1}, \tag{3}$$

where, c is the speed of light in vacuum. The electron plasma frequency is close to the Langmuir wave frequency and it is given by [101]

$$\omega_{plasma} \approx \omega_e = \sqrt{\frac{4\pi n_e e^2}{m_e}} = 5.6 \times 10^4 \sqrt{n_e\ cm^3}\ sec^{-1}, \tag{4}$$

where ω_e is the electron plasma frequency and n_e is the density of electrons in the plasma, given in cgs units. The propagation of laser pulses is supported by plasmas only if the plasma frequency is lower than the laser frequency [35]. For the seed pulse to propagate in a plasma, the following condition must be satisfied [101],

$$\omega_{seed}^2 = \frac{4\pi e^2 n_{cr}}{m_e}, \tag{5}$$

and the critical number density of the plasma, n_{cr} is given by [101]

$$n_{cr} = \frac{\pi m_e c^2}{e^2 \lambda_{seed0}^2}. \tag{6}$$

2.2. Factors Limiting Raman Amplification

2.2.1. Forward Raman Scattering (FRS)

The FRS instability of the pump is one of the primary drawbacks of existing backward Raman compressors and amplifiers [100]. In gases, FRS typically grows more quickly than the backward instability. The efficiency of the laser pulse compression by backward Raman scattering is severely constrained by the adverse forward-to-backward asymmetry of Raman gain.

2.2.2. Langmuir Wave Breaking

The energy fraction, $\frac{\omega_{plasma}}{\omega_{pump}}$ (the energy lost by the laser pump) is acquired by the Langmuir wave in the aforementioned resonant three-wave decay process. This process takes place at a specific spatial location for a short period of time which is equivalent to the duration of the amplified pulse as it passes through the plasma [101]. The Langmuir wave keeps the acquired energy for this duration, assuming no damping happens in such a short period. The transmission of pump energy to the backward propagating seed is facilitated by the Langmuir wave and this continues until the Langmuir wave can contain this energy. However, the phenomenon of wave breaking restricts the energy density of the Langmuir wave that can be supported by the plasma. When the electron quiver velocity in the wave approaches the phase velocity of the wave, the Langmuir wave breaks. This phase velocity of the wave is given by [101]

$$v_{phase} = \frac{\omega_{plasma}}{k_{plasma}} \approx \frac{c\,\omega_{plasma}}{2\omega_{pump}}. \tag{7}$$

At wave breaking, the Langmuir wave energy density is given by [101]

$$D_{langwb} = \frac{n_e m_e v_{phase}^2}{2} \tag{8}$$

and the energy density of laser pump at the limit of wave breaking is given by [54]

$$D_{pump} = D_{langwb} \frac{\omega_{pump}}{2\omega_{plasma}}. \tag{9}$$

From this equation, it can be inferred that the pump slice losing energy within a specific plasma layer is twice as thick as this layer, which accounts for the factor 2 in the denominator. Consequently, the pump intensity at the Langmuir wave breaking threshold can be expressed as [101]

$$I_{wb} = cD_{pump} \approx \frac{n_e m_e c^3 \omega_{plasma}}{16\omega_{pump}} = I_m \left(\frac{n_e}{n_{cr}}\right)^{3/2}, \tag{10}$$

where $I_m \approx \frac{n_{cr} m_e c^3}{16}$. When the conventional three-wave decay mechanism is considered, only a fraction of the pump energy (I_{wb}/I_0) is consumed at pump laser intensities greater than the wave-breaking threshold ($I_0 > I_{wb}$) [54]. As a result, backward Raman amplification regimes where $I_0 < I_{wb}$, described by the hydrodynamic or fluid description, must be considered to prevent Langmuir wave breaking.

2.2.3. Other Factors Limiting Raman Amplification

It is crucial to note that the archival literature goes into considerably more detail about both the adverse consequences discussed in this quick guide and those that are not. These include the production of superluminous precursors of the amplified pulse [102], pulse scattering by plasma density inhomogeneities [103], and parasitic effects of plasma noise on the Raman scattering of the pump and amplified pulses [29,54,58,104–106]. By choosing the right seed parameters, such as the seed duration, intensity [107], and the chirp of the seed [57], advantageous compression regimes are achievable. Additionally, the effect of relativistic electron nonlinearity on filamentation and detuning of amplified pulses are explored in detail [108–110]. Additionally, a detailed description of the robust operating regimes in density-temperature space has been provided [111]. Pulse depletion and plasma heating by inverse Bremsstrahlung are the two other topics discussed [112–117] with regards to this topic.

2.3. Mitigating the Limiting Factors of Raman Amplification

Over the past three decades, a great deal of research has been done on SRS in plasma [118–120]. The initial driving force for research was the need to comprehend the parametric instabilities that appeared in laser-driven fusion tests [76]. Raman amplification is only observed below the density ratio $n_0/n_{cr} < 0.25$ and it is forbidden for the energy densities beyond this value. There are linear and nonlinear regimes for Raman backscattering (RBS) amplification [121]. The gain is independent of the seed intensity in the linear domain and the pump depletion is minimal. Pump depletion and the accompanying temporal compression of the amplified pulse define the so-called "pulse regime", which is a nonlinear regime. In this domain, Raman amplification and compression of ultrashort pulses in the plasma allows intensities to reach 10^{20}–10^{21} W/cm^2 in a small laboratory-scale device and an unmatched intensity of 10^{25} W/cm^2 using PW-class lasers [122]. Such intensities open new research directions and results in useful applications such as laser wakefield accelerators, X-ray lasers, or fast ignition for inertial fusion [123].

Even though earlier studies related to Raman scattering aimed at understanding the instabilities occurring in the laser-driven fusion experiments [76], SRS improved the understanding of the process, leading to the establishment of a potential compact plasma-based amplifier/compressors that could provide PW laser powers [124]. Two regimes—the linear regime and the wave breaking regime are considered in SRS, whereas the linear regime of SRS is considered unsuitable for the amplification of ultrashort and ultraintense pulses due to pulse lengthening [29] and autoresonance [125], the wave breaking regime is potentially suitable for obtaining ultrashort, ultraintense laser pulses [126]. Investigations on the FRS of short-pulse relativistic-intensity laser pulses was carried out by deriving the differential equations that models the instability for a large pump and shows that the growth rate asymptotically approaches zero for ultrarelativistic intensities under some relevant conditions. The two initial conditions considered in [92] shows that there is an amplification of any noise by a factor of 10^4. Reports on the measurement of the Raman backscatter produced by laser plasma interaction where the laser focal profile of the beam was smoothed by induced spatial incoherence (ISI) showed substantially less Raman backscatter than when a regular beam (without any smoothing) was used [127]. The commencement of the Raman scattering produced with an ISI smoothed laser beam was predicted well by a convective model that accounts for the instantaneous focal pattern. The backscattering measurements from plasmas produced by a short wavelength (351 nm) laser show clear thresholds and low-level saturation for the two plasmon instability, as well as for the absolute and convective Raman instabilities. The convective Raman instability occurs over a density range of $0.2n_c$ to $0.5n_c$, and the scattered light spectra indicate the steepened density profile at the quarter critical density [82].

The relevance of stimulated scattering in backward and forward directions and self-modulation for an intense laser beam propagating in a plasma is assessed under conditions that are expected to be optimum for a plasma compressor. Two-dimensional simulations for calculating the small gain of the stoke pulse for various plasma parameters revealed that these processes should not seriously deplete the pump beam energy if the scattered waves are initially at the noise level, for the plasma compressor condition, and the self-modulation and filamentation does not alter the spatio-temporal qualities of the beam [128]. Later, amplification due to SRS was theoretically investigated by different research groups around the globe. All these investigations mainly used the three-wave interaction model and the PIC simulations for understanding the phenomenon behind SRS. Different effects such as wave breaking, field generation, and Landau damping limits Raman amplification [115]. However, the intensity obtained by Raman amplification, is limited to 10^{17} to 10^{18} W/cm^2 in these cases. Beams with larger unfocused beam diameter when focused to a small focal spot of the order of a few μm to tens of μm, can enhance the capability of Raman amplification to achieve intensities of the order of 10^{22} W/cm^2, which are important when considering experiments in the relativistic regime [100]. However, this may lead to effects such as filamentation and self-focusing. A simple three-wave model and PIC code was used to study Raman amplification away from wave-breaking and particle-trapping regimes [129]. The three-wave model is in good agreement to a fully kinetic PIC code for a particular peak probe intensity. The three-wave model allows simple calculations, and it allows us to modify a relatively reduced calculation compared to the PIC. The three-wave model also allows us to include effects like heating (reducing pump depletion without significantly reducing the probe amplitude) and collisional effects, with reduced efforts, whereas the PIC codes in general do not include these type of effects. A new theoretical model for the interaction between two counter-propagating laser pulses in an unmagnetised plasma was put forward by a group of researchers in 2009 [130]. Pulse compression and pulse-amplification mechanisms are explored through a one-dimensional fluid model for RBS. Amplification is obtained by transferring energy from a long pump pulse to a short seed pulse via the Langmuir plasma wave. In this theoretical model, changes in amplification were observed in accordance to the intensity profile of the pump pulse. A Gaussian and a ring intensity profile were considered in the simulations, wherein a highly certain intensity profile of the pump laser having a moderate total power, played an important role to provide better compression and amplification. A 50-fold pulse compression and greater peak power was obtained in these simulations, allowing the realization of a table top amplifier with peak intensities which are far beyond the abilities of the current CPA-based amplifiers [130].

The variation in the output intensity of the Raman amplifier due to FRS, modulational instability and Langmuir wave breaking are studied by using PIC simulation with Zohar code and a method of using intense seed pulse to simultaneously photo-ionize the plasma with its amplification was described in [131]. It was found that for an electron temperature, T_e = 200 eV, plasma density lies between the threshold predicted in [132] and the breaking threshold for a cold plasma [131]. A saturation amplification was obtained at an intensity of $\sim 10^{17}$ W/cm^2 at the optimal plasma density. The obtained amplification was in the form of the amplified pulse breaking into two lobes and a ceasing pump depletion. It was also verified that the seed achieves its maximum amplification when operating near the wave-breaking limit and the seed amplification decline quickly with declining density. The characteristics of the laser amplification by SRS and pulse compression characteristics during the amplification process was formulated by using a 1D fluid model [133]. Amplification is achieved through two stages i.e., by linear and nonlinear regimes in which the peak amplitudes grows exponentially and linearly respectively. The time evolution of compression of the first half of the seed and the rear half shows that broadening and compression phases are common but their behaviours are distinct. These results indicates that the efficiency of amplification is larger for the larger pump intensity and higher plasma density [133]. Furthermore, it was reported in [113] that powerful laser pulses could be effectively compressed through backward Raman scattering in plasmas with densities similar to low-density solids, i.e., $\sim 8.2 \times 10^{20}$ cm^{-3}. This work numerically examines the regions where the damping is strong (known as the quasitransient regime) with a simple model that considers major effects like RBS, relativistic electron nonlinearity, and Landu damping, indicating that the compression of powerful laser pulses in ionized low-density solids can be highly efficient [113]. Another investigation on the basis of a three-dimensional three-wave interaction model revealed the details of the transverse filamentation for seed pulse propagation in the π limit [68]. Reducing unnecessary plasma processes during the generation of ultraintense, ultrashort laser pulses by parametric processes in plasma leads to operational limits explained by filamentation. The applicability of three-wave interaction model is discussed by comparing 1D pulse forms with those obtained from 1D PIC simulations and Vlasov simulations. Kinetic simulations show that the leading pump pulse creates situation similar to those obtained from three-wave interaction model even though wave breaking happens. Vlasov simulations [134] show that wave-breaking criterion does not cause much disadvantage to the filamentation-free leading pulse propagation because the first pulse of the π pulse is more affected by the succeeding oscillations than the wave-breaking criterion. PIC simulations also supported the investigations on Raman amplification and compression of nanosecond (ns) laser pulses to ps duration [106]. The optimal pump and probe durations were found to increase with decreasing pump intensity for a constant pump-to-probe compression ratio. In addition to this, the relative importance of the undesirable instabilities remains the same (pump RBS and probe FRS) or even decreases (filamentation and modulational instability) with decreasing pump intensity. It was also found that the energy transfer efficiency of up to 60% was achieved, thereby allowing the Raman amplification in plasma to produce ps pulses with large energy and moderate intensity. Such pulses can be widely employed for a variety of high-energy density physics applications, including fast-ignition inertial confinement fusion [135] and radiographic diagnosis of dense plasmas by using X-rays and protons [136]. The first large scale multidimensional PIC simulation of the Raman amplification process predicted the ability to achieve multi-PW powers by using Raman amplification [59]. This technique is scalable at short wavelengths, allowing the compression of X-ray free electron laser pulse to attosecond duration. From these simulations, in general, it was discovered that more effective amplification results from raising the pump intensity and/or plasma density. However, this will also induce the growth of unwanted instabilities of both pump and seed and leading to reduced focusability. These issues narrow the parameter windows for effective Raman amplification. However, a parameter regime in which a 4-terrawatt (TW), 700 μm FWHM, 25 ps laser pulse at 800 nm can be amplified to 2 PW peak intensity with 35% efficiency was reported in [59]. A theoretical simulation using 3D PIC simulation showed that SRS can generate and amplify twisted pulses to PW intensities in plasma [124]. The final intensity of the seed pulse of the order of 10^{17} W/cm^2 and the seed laser spot size of the order of 1 mm, indicates the production of PW class twisted laser with orbital angular momentum (OAM). Simulations showed that the Raman amplification can also operate in the absence of exact frequency and wavenumber matching between the seed and pump as long as the seed is short enough for its Fourier components to still satisfy k-and-ω matching conditions [124]. An alternate method to use plasma wave seed instead of counter-propagating laser seed in Raman amplification was proposed in 2017 [74]. Here, the seed pulse and the plasma wave (Langmuir wave) produces the same output as that of counter-propagating waves. It was found that in the nonlinear regime, for the corresponding laser seed, the output pulse reaches self-similar attractor solution [55]. Chirping the seed pulse frequency provides the same efficiency as chirping the wavelength of the plasma wave. The proposed method provides a great experimental advantage because it avoids the production and synchronization of the frequency shifted laser seed. This technique assures that the new method is a good alternative for implementing high-intensity laser compression in plasma with a specific advantage concerning the timing of the pulses. The Raman seed pulse amplification in 1D backscattering geometry using numerical simulations and analytical calculations were investigated elsewhere [64]. The results of three-wave interaction acquired from the PDE2D code [64] was compared with the new Vlasov code. For the linear stage of amplification, there is a lower limit for the pulse width of the seed for direct amplification. The smallest possible pulse width of the seed depends on the pump strength and the plasma density. With a fixed plasma density, the pulse produced during the initial period will be further amplified and may develop into a self-similar pulse solution in the nonlinear (pump depletion) regime [64]. Experimental investigation on the effect of chirp of the pump on Raman amplification is presented in plasma [137], where the chirp of the pump leads to a spatio-temporal frequency distribution of the gain. The effective interaction length was restricted to $\pi \mid \gamma_0/2\alpha \mid$ and gain was proportional to pump intensity. The measured scaling was corroborated to the evidence that super-radiant growth of the seed pulse occurs in a linear chirped pulse Raman amplifier. In view of this research, it can be inferred that chirped pulse Raman amplification (CPRA) is capable of controlling the amplification process from Raman linear regime to the Raman nonlinear regime or Compton regime, and it has the potential to serve as a high-efficiency, high-fidelity amplifier/compressor stage for high-power laser amplifiers.

Unprecedented ultra relativistic laser intensities can be achieved by compressing a powerful laser pulse by using backward Raman amplification (BRA) in plasma, followed by vacuum focusing to a small spot size [100]. Inhomogenity in the plasma density during BRA causes laser phase and amplitude distortions, limiting the focusibility of the pulse. Using a phase conjugated laser pulses helps to maintain the focusability in the nonlinear pump depletion regime of BRA [138]. Noise suppression and enhanced focusability in the plasma Raman amplifier with multi-frequency pump was reported elsewhere [139]. Amplification by resonant RBS in plasmas represents one of the most promising ways to generate ultraintense short laser pulses. According to numerical calculations, additional chirping of each of the beams mitigates Raman instability and these findings propose ways to implement the plasma Raman amplifier by using the multiple-beam pump. First, in uniform plasma, temperature fluctuations and seed precursor instabilities have little impact on focusability. Two beams with a frequency difference of $\Delta\omega \approx 0.1\gamma$ are already enough, as demonstrated by numerical simulations [139], to prevent large-scale speckles in the pump construction and offer nearly optimal focusability with $\eta > 90\%$ efficiency. The second reason for using multiple-beam pumps is to decrease plasma temperature variations. A large number of beams are needed to disperse pump energy over a wider bandwidth, which scales as $1/\sqrt{N}$, and limits Raman instability. Distributing pump energy over a wide bandwidth may cause poor absorption by the intended signal, resulting in inadequate amplification. Seven to ten beams scattered over the spectral width $\Delta\omega \approx N\gamma$ were found to restrict thermal fluctuations while retaining signal amplification gain. Moreover, if a strong seed is utilised in the beginning of contact, the number of beams and pump bandwidth can be enhanced. It was also found that tuning the chirp of the pump can improve Raman amplification of undesired signals if the optimal chirping parameter (q) is not too high and enough chirping is provided to stabilise plasma temperature fluctuations and parasitic seed precursor amplification. Given these limits, the optimal chirping parameter is $q \leq 0.1$, which is substantially lower than the value expected for homogeneous plasma. In light of all the findings, a mixed pump that superimposes laser beams with slightly varied frequencies is suggested as a promising method for amplifying ultra-intense laser pulses by RBS. Even with thermal fluctuations and seed precursors, a mixed pump is found to transmit $\sim$50% of the entire energy of the pump beam into the amplified pulse.

Investigations into the wave-breaking regime of Raman amplification are significant for increasing the intensity of a laser pulse [126]. Earlier studies of the Raman amplification reveals that the conversion efficiency would increase until the wave-breaking threshold, after which an increase of the pump intensity results in a decreased efficiency. Previous analytical predictions, Vlasov–Maxwell simulations and PIC simulations were compared in [126] by using a new 2D PIC simulation. This reveals that when the pump intensities go over the wave-breaking barrier, conversion efficiency drops monotonically. The effect of heating in the wave-breaking regime was investigated by using a three-wave model, leading to the identification of new regime in which a probe pulse may be compressed and amplified without significantly depleting the pump because of a shift in plasma resonance caused by heating the plasma. In the damping-dominant regimes, inverse Bremsstrahlung dominates at high densities and plasma preheating can increase the growth rate. Thermal effects can reduce the maximum achievable effciency due to a decreased wave-breaking limit at a finite temperature [115]. The coherent wave-breaking (CWB) regime of Raman amplification was identified in [140], where amplification occurs after the start of wave breaking and before the destruction of coherent coupling between the seed, pump and plasma wave due to phase mixing. Due to this, the amplification in this region has a transient effect. The CWB regime can be accessed by using short and intense seed pulses. The parameter scans reveal a clear distinction in behaviour between the below wave-breaking regime, where energy transfer efficiency is high but total energy transfer is low, and the wave-breaking regime, where efficiency is low, and CWB, where moderate efficiencies allow highest total energy transfer. Laser compression by SRS in a plasma with a time span compared to the time needed for the filamentation instabilities to occur was reported in [54]. The optimum regime for pulse amplification is the near-threshold region, which combines the maximum possible energy with maximum possible efficiency. At the wave-breaking limit, the compression efficiency can reach up to 100% [54]. This method reduces the costs related to building an ultrahigh-energy laser because large energy fluxes without beam filamentation can be sustained in this regime.

Generally, the seed pulses used in Raman amplification does not have enough intensity to reach the nonlinear optical regime. Consequently, there will be a longer stretch of an inefficient linear regime for the amplifier [137,141]. Following the method suggested in [142], this can be rectified by commencing amplification at focus where the seed effectiveness is maximum. The new geometry proposed increases the allowable pump energy keeping the seed pulse requirements unchanged and eliminates the difficulties in the seed ionisation scheme. This geometry utilises a multi-kilojoule pump pulse with sub-millijoule seed pulse to obtain very high pulse powers with only FRS and filamentation of the amplified pulse as limitation. In this scheme, a seed pulse of 0.3 mJ was amplified to $\sim$1.2 J, where FRS and filamentation were the only limitations. The progress on developing a plasma amplifier/compressor based on Raman scattering was reported in [62]. Here, a millijoule seed pulse was generated by using an external Raman gas cell, and the generated seed pulse was redshifted. To eliminate the angular spray of the amplified seed, the upper limit of the pump intensity is determined by the interaction between the shifted ps seed pulse and the ns pump pulse in a gas jet plasma. Raman amplification in this work was considered to be a function of pump and seed intensities. Even though the Landau damping was present, amplified pulse of energy up to 14 mJ was demonstrated. Saturation of amplification was detected when the seed energy was increased. PIC simulations shows that the saturation effect can be used to minimise the RBS loss for multiple crossing beams and the simulations also suggested that shorter seed pulses will be more helpful for overcoming the saturation and for efficient laser amplification and compression [62]. A 25 ps, 4 TW laser pulse was compressed to 25 fs, 1.5 PW by using PIC simulation [143], and for these optimal parameters, Raman amplification was supposed to be extended to centimeter-wide spot size, allowing the generation of 300 PW laser pulses as short as 30 fs.

Raman processes were also reported in various reports involving laser wakefield acceleration (LWFA). The stimulated Raman side scattering (SRSS) (which occurs at the beginning of the laser–plasma interaction, contributing to the evolution of pulse before the formation of wakefield) of an ultrashort high-power laser and the relativistic shift in plasma frequency was investigated in the plasmas created in LWFA [93]. The electron beam quality is decreased due to the excessive involvement of SRSS. A spatially resolved measurement of the intensity of the laser upon propagation through plasma indicates a prominent Stokes shift due to SSRS. SSRS contributes to reshaping the laser pulse to the matched pulse duration. It was found in this investigation that an improved focal spot quality, which is comparable to the matched spot, can increase the beam quality. Simultaneous measurements on high-energy electrons and plasma wave characteristics had been conducted in a self-modulated laser-wakefield accelerator, where acceleration of 10^8 electrons up to an energy greater than 1 MeV with a peak energy of approximately 30 MeV was observed from the background plasma [144]. A strong relation between the amplitude of the plasma wave and electron production with evidence of wave breaking was observed in this experiment, in which the electrons were accelerated in a self-modulated LWFA (SM-LWFA) at a relatively low power (2.5 TW). The optical diagnostics in the experiment indicated the presence of highly nonlinear, large amplitude plasma waves. The numerical simulations showed that the plasma electrons are pre-accelerated to a sufficient energy to be trapped by the high-phase velocity wakefield by the low-phase velocity beat waves generated by RBS. Both simulation and experiment shows that the acceleration and trapping of electrons heavily depend on the wakefield amplitude [144].

Raman amplification has great importance in the scientific field not just for amplification purpose but also other applications such as beam cleaning in plasma [144]. If the correlation time of the pump laser is longer than the inverse plasma frequency, backward Raman amplification in plasma can effectively compress a temporally incoherent pump laser into an intense, coherent amplification seed pulse. The noise-seeded instabilities such as filamentation and spontaneous scattering can be suppressed by the use of a moderately incoherent pump and this indicates that parametric plasma amplification with quasicoherent sources like free electron lasers (FELs) is technically possible and a means of enhancing the coherence of X-ray sources. Compared to SRS in the linear regime, Raman amplification is far more robust to incoherence and enables amplification to relativistic intensities with pump correlation times on the scale of the inverse plasma frequency. The robustness of Raman plasma amplifiers and the scheme of creating attosecond pulses from RBS in under-dense plasma was investigated in [145]. The output $\sim$300as with energy similar to the fourth-generation sources were created in the PIC simulations used in these investigation. Amplifying ultrashort laser pulses (200 fs) in microcapillary plasmas by counter-propagating pumping beam was reported in [146], where a 5 times increase in energy was observed. The parameters of this experiment support not only the amplification of the pulse but also an utterly rising instability, if the pump is not exhausted. Hence it is crucial to have entered a nonlinear pump depletion regime. In order to differentiate the anticipated spatio-temporal pulse evolution in this regime, there was not enough time resolution and evidence of pulse intensities that were significantly higher than the pump intensities. Non-ideal effects, such as defocusing, density inhomogeneities forcing the interaction off resonance, or damping effects, continue to make it difficult to develop a quantitative theory. Hence, this experiment is viewed as a first step toward showing how an ultrashort pulse might enter the pump depletion phase. It was demonstrated that the amplification decreased as the energy of the seed pulse increased because there was very little pumping energy available during this brief time window. Additional research on micro capillaries $\sim$200 mm long confirms the hypothesis of short interaction lengths, and the findings indicate agreement between the observed amplification and the linear growth rate [147]. Therefore the studies suggest that spatial impacts, both transverse and longitudinal, must be taken into account as interaction length increases. The preplasma must be completely ionised or have an ionization level high enough for the pumping pulse to ionise in order to eliminate problems such as ionization-induced defocusing. It would also be necessary to guide the laser pulses if the interaction length was more than the Rayleigh length, making the laser-produced plasma in microcapillaries inapplicable for amplifications. In Raman amplification experiments, alternative plasma-generating techniques such as discharges and laser sparks can also be used [147]. RBS and amplification was demonstrated in a gas-jet plasma [148]. Plasma density gradients can sometimes widen the band width of the RBS, which is constrained to double the linear growth rate. It has been noted that a 500 fs counter-propagating seed pulse is amplified by a factor of two. Two significant changes were introduced to the experimental setup from the previous microcapillary investigations mentioned in [147], enabling simultaneous plasma density measurements for the Raman resonance by swapping the microcapillary plasma for a high-pressure gas jet plasma and lower plasma density. The matching density is reduced by more than an order of magnitude, and the inverse Bremsstrahlung absorption ($\propto n_e{}^2$) is decreased by two orders of magnitude by using a new pair of laser wavelengths. Hence the laser pulse damping is significantly reduced as compared to the microcapillary experiments. Amplification via gas-jet plasma ($n_e \approx 1.3 \times 10^{19}\,\mathrm{cm}^{-3}$) and microcapillary plasmas ($n_e \approx 1.1 \times 10^{20}\,\mathrm{cm}^{-3}$) produced an amplification of up to eight and two, respectively. The inhomogeneity of the plasma density was the main cause of the low amplification. The experiment was refined further by increasing the seed intensity, fine-tuning the spatial and temporal overlap between the seed and pump, and increasing the axial uniformity of the plasma density in order to produce greater amplification. By using the resonant Raman (occurring at the corresponding wavelength with different plasma densities) technique in a gas-jet plasma, it was found that short laser pulses can be amplified up to 95 times. The bandwidth of the amplified pulse widens as it is amplified. Shorter output pulses lead to more amplification, as per the pulse duration measurements with a single point autocorrelator. To show resonances at various densities, a broad-bandwidth seed was used. Substantial amplification is an important step toward achieving the nonlinear depletion regime and, ultimately, a workable technique for amplification of ultrashort laser pulses, even if the observations in [60] have not yet confirmed the onset of the nonlinear depletion regime.

Superradiant amplification (SRA) of ultrabrief laser pulses was demonstrated for the first time in [149]. The term SRA suggests that the pump pulse is coherently backscattered by all involved plasma electrons. The SRA mechanism is appealing as the last amplification stage of a CPA laser system because of the excellent focusability of the amplified signal pulse. A weak input signal pulse is initially amplified in the Raman regime until its strength rises to the point at which it enters the SRA regime, according to the results. By tightly focusing both pulses, the input signal intensity can be increased, thereby approaching the SRA regime in a short span of time. The amplification begins within the short Rayleigh length and moves into the diverging beam in this method, dispersing the energy over a larger area while maintaining the intensity below the relativistic level, making this technique suitable to attain PW powers. A counter-propagating fs laser pulse and a frequency-modulated broadband pump pulse with the same carrier frequency are used in an experimental demonstration for amplifying a fs pulse via SRS in a dielectric capillary filled with gas plasma [150]. The increase in spectral intensity by a factor of 10^3 and output energy ratio by a factor of 10^2 were the values obtained for amplification at the time of these investigations. The high level of pump-frequency modulation and plasma wave breaking prevented the utilization of the benefits of the capillary waveguide and achieving the nonlinear amplification regime with a high gain in their experiment. By lowering the pump-frequency modulation level and detuning the seed and pump carrier frequencies, the negative effects of these parameters were significantly decreased. As a result, the plasma concentration and, consequently, the plasma wave-breaking threshold, was raised. Therefore a hydrodynamic mechanism for plasma-wave breaking was suggested as the mechanism playing a significant role in the amplification restriction in the scheme under consideration based on experimental data and the outcomes of theoretical calculations.

Previous studies showed minimal amplification in gas-jet plasmas and short microcapillaries [147,148]. Recently, a plasma produced in a 2 mm long gas jet with an effective (i.e., with the right density) plasma length of ≈1–1.5 mm was shown to have an energy amplification of almost 100 times [60]. Amplification of energy up to ∼100 times [150] was observed in similar experiments, wherein the results were partially attributed to Compton scattering [151]. However, the vast majority of the amplification, appears to be in the resonant domain, as in other early investigations. It was reported that the Raman backscatter interaction in a 2-mm-long gas-jet plasma increased the strength of a sub-ps laser pulse by a factor of up to 1000 [123]. The intensity of the amplified pulse was more than an order of magnitude greater than that of the pump pulse as Raman amplification entered the nonlinear region. Gain saturation, bandwidth broadening, and pulse shortening features peculiar to the nonlinear regime were reported. The results were qualitatively consistent with simulation and theory. Successful improvement in the efficiency of the amplifier system was reported in [63]. A total of 6.4% of energy was transferred from the pump to an ultrashort pulse (50 fs), which was higher by a factor of 6 than previous reports [60,123] had found. To achieve this, a plasma with a sizable density gradient and a double-pass design was used to produce an unprecedentedly huge intensity amplification of nearly 20,000 times in a plasma of just 2 mm in length [123]. Additionally, this method not only enables the short pulse to draw more energy from the pump but also to continue compressing it to achieve very high output intensities, for instance, from 500 fs down to 90 fs in a single pass and even lower to 50 fs in a two-pass experiment [63]. In fact, intensities of the order of 10^{24}–10^{25} W/cm^2 is theoretically possible by employing a much larger pump laser and plasma (i.e., plasma with greater diameter and length) [54,152].

Even though several improvements in SRS were achieved, no experimental evidence of SRS was available for investigations on using a plasma waveguide for amplification of laser pulses, until its first appearance in [141]. Amplification of more than 900 times was reported when a 9 mm plasma waveguide was employed. However, the main challenges of using a plasma waveguide as an amplifier are the restrictions on the pulse duration and heating of the waveguide caused by the pump pulse. If the SRS regime is achieved, both restrictions may be relaxed as frequency matching is not necessary for SRS. On the other hand, the ability of the pump pulse to taper the on-axis density can be used to inhibit the near-FRS [105] of the amplifed seed pulse and the superluminous precursor [102] in a high-power amplifier. Pumps with ns pulse duration are prone to instabilities, such as filamentation, resulting in beam spray [153], due to the longer laser-plasma interaction time and reduction in the optical quality of the amplified pulse. The Raman scattering growing from thermal noise caused by these ns pumps also competes with the seed pulse. Even in a plasma amplifier designed for heating the plasma by using a ns-long pump results in significant Landau damping of the plasma wave. Understanding the coupling of multiple laser beams in inertial confinement fusion experiments, where the individual beams undergo SRS in the target interior, and the associated scatter can further be amplified as it crosses other beams after exiting the target, requires research on Raman amplification in a high-temperature plasma with strong Landau damping [154].

Raman amplification in a reasonably hot plasma with dominant Laudau damping using a ns pump pulse was demonstrated in [62]. As the seed energy rises, amplification approaches saturation. PIC simulations indicate particle trapping as the mechanism is compatible with the saturation. The loss via RBS of the numerous crossing beams employed for the indirect drive ignition of fusion processes may be reduced because of this saturation effect [154]. A shorter seed pulse may also be useful to get past the observed saturation and enable more effective Raman amplification and compression of laser pulses, according to the PIC simulations. In a Raman plasma amplifier, the goal is to produce plasma conditions where RBS is the fastest-growing instability, outpacing all rival effects such that, by leveraging that instability, a laser beam can be amplified and compressed to ultrahigh unfocused intensities. However, experimental results show that using this approach to achieve high efficiency is quite challenging. According to recent findings, SRS, SBS, and stimulated electron-acoustic scattering (SEAS) all occur simultaneously [155]. It is difficult to explain the presence of SEAS without noting the interaction between SRS and SBS. SEAS is a sign of substantial particle entrapment [155]. Raman amplification of short seed pulses with various chirp rates were examined in [156] by employing a chirped pump pulse in a plasma waveguide. The experimental findings were supported via PIC simulations, where slowly fluctuating amplitudes were considered. Electron entrapment and wave breaking were observed when the seed energy reaches several millijoules over periods of tens to hundreds of fs for 250 ps, 800 nm chirped pump pulses. These key saturation mechanisms result in spectral broadening and gain saturation. This also limits efficiency and inhibits access to the nonlinear zone. Observation and measurement of SRS occurring via the interaction between a large underdense, preformed plasma and an intense sub-ps laser pulse was investigated in [95]. The results were in agreement with the theory of the time-integrated reflectivity [157]. As the intensity of the interaction beam approaches 10^{16} W/cm^2, the SRS reflectivity increases and saturation was observed for the values greater than 10^{17} W/cm^2. These results suggest that short pulse driven SRS can be explained by the linear theory of three-wave parametric instabilities arising from thermal equilibrium noise [158]. Amplification of a 1 mJ, 1 ps, 1200 nm seed laser by a 30 J, 12 ns, 1054 nm pump beam in a low-density plasma was reported in [159]. When the plasma is close to the resonant density for SRS (compared to the measured transmissions at wavelengths just below the resonant value), the transmission of the seed beam is increased $\sim$25 times and amplification increases with increasing the pump intensity and plasma density. The simultaneous amplification and compression of an input pulse by using SRS in a millimeter-scale plasma to increase its intensity by more than two orders of magnitude is described in [63], where a double pass provided more amplification and compression of seed pulses. This method can be easily expanded upon in the future with a multi-pass, cavity-like architecture, making it possible to create a brand-new generation of ultrahigh-intensity laser systems that are compact and affordable.

3. Stimulated Brillioin Scattering (SBS)

3.1. Theory

A three-wave coupling interaction between two electromagnetic waves and an ion-acoustic wave is referred to as SBS [160]. This is equivalent to the process in which an incident laser photon (frequency = ω_{pump} and wavenumber = k_{pump}, respectively) decays into an ion-acoustic wave (phonon) (with frequency = ω_{IAW} and wavenumber = k_{IAW}), and a scattered photon (with frequency = ω_{seed} and wavenumber = k_{seed}), which moves roughly opposite to the direction of the incident laser [161]. It is evident here that the effective transfer of energy in this process involves frequency and wavenumber matching requirements given by [50]

$$\omega_{pump} = \omega_{seed} + \omega_{IAW} \tag{11}$$

$$k_{pump} = k_{seed} + k_{IAW}. \tag{12}$$

SBS is an instability that amplifies both the scattered wave and the system's inherent low-frequency mode [162,163]. However, the presence of an incident electromagnetic pump wave significantly alters the acoustic mode for sufficiently strong electromagnetic waves, as in modern laser-plasma interaction experiments relevant to laser fusion [163]. This happens for intensities where ω_{IAW} is greater than the traditional growth rate, i.e., γ_0. Thus, stimulated scattering in this regime is known as SBS in the strong coupling mode or quasimode (sc-SBS) [164,165]. The modified low-frequency mode involved in the three-wave process is not a natural mode of the system without the pump wave; hence the term quasimode. The collective ion-acoustic wave serves as an intermediary in weak coupling (wc-SBS), whereas a driven mode is responsible for energy transmission from pump to seed in strong coupling. The equation for density perturbation (where the weakly coupled and highly coupled Brillouin scattering models diverge) is described by the three-wave interaction. The plasma density equation contains a first-order time derivative in the weak coupling regime, whereas a second-order time derivative is present in the strong coupling regime. Reaching the nonlinear stage, where the amplitude and width of the seed are driven by a self-similar behaviour, is a crucial issue for both amplification strategies [66,166,167].

The ponderomotive force (given by $F_p = \frac{-e^2}{4m\omega^2}\nabla(E^2)$) produced by counter-propagating laser beams drives the charged particles to regions of lower intensity in a light field with a slowly varying envelope [168]. Here, ω is a high-frequency oscillation, E is the strength of the electric field, and e and m are the charge and mass of the particle, respectively. Although both ions and electrons are affected by the ponderomotive force, the changes in ion density arise from the response of the ions to the electrostatic field of the displaced electrons [168]. The electrostatic force on the ions is m_i/m_e times greater than the direct ponderomotive force because it is equal to the electrostatic force on the electrons, which should balance the ponderomotive force on the electrons [168]. As a result of this pondermotive force, the ion and electron densities fluctuate at a frequency equal to that of the difference between the pump and seed laser frequencies [168]. Although both electrostatic and pressure factors can affect the ion-acoustic waves in general, the electrostatic factors dominate for SBS and the pressure factors are disregarded as it is negligible compared to the electrostatic term [168]. By modulating the transverse current caused by the pump and scattering energy into the seed, the resulting electron density variations also provide an amplified seed pulse with a centre frequency that is lower than that of the ion accoustic wave. Both the seed and the density fluctuations evolve over time because the seed drives the density fluctuations intensely as it grows. The density fluctuation can only be described as a wave if the wavelength is less than the regime being considered, the duration of SBS is constrained by the period of the ion-acoustic waves [168], or in the case of sc-SBS, the period of the quasimode [168]. The highest intensity and minimum pulse duration attained in practical systems are constrained by the emergence of other instabilities such as FRS, filamemtation etc., as discussed in Section 3.2 [66,169].

3.2. Factors Limiting Brillouin Scattering

It is important to consider the factors limiting Brillouin scattering in the context of amplification of laser pulses as it helps in optimising the respective laser and plasma parameters to attain higher amplification ratio. With regard to this, effects of the resonance state, filamentation, and forward Raman scattering [66,169] are evaluated and summarised in the following sections. The laser beat drives a low frequency ion mode in Brillouin amplification schemes. Amplification can either be wc-SBS or sc-SBS. The driven plasma mode in the strong coupling (sc) as opposed to the weak coupling (wc) Brillouin scenario is a quasimode with a significantly higher frequency compared to an ion acoustic wave. wc-SBS always occurs in the plasma density regime $n_0/n_{cr} < 0.25$ [168]. However, for strongly coupled Brillouin amplification, two plasma density regimes can be considered (i) $n_0/n_{cr} > 0.25$, referred to as greater than subquarter-critical density and (ii) $n_0/n_{cr} < 0.25$, referred to as less than subquarter-critical density. Here, n_0 and n_{cr} are the density of plasma electrons and the critical density (i.e., density at which the pump beam can no longer propagate), respectively [170]. These regimes are differentiated from each other by understanding the instabilities arising during amplification via Brilloiun processes. Although a reduction in the growth of instabilities such as filamentation [111] is observed for $n_0/n_{cr} < 0.25$, SRS is prohibited in $n_0/n_{cr} > 0.25$ [171], eliminating a broad range of instabilities that prohibit amplification. In addition to this, larger plasma densities facilitate a quick growth in SBS, causing a quick rise in the Brillouin-amplified pulse and hence an increase in the compression ratio leading to amplification [60]. The factors that can degrade amplification via Brillouin processes are discussed below.

3.2.1. Forward Raman Scattering

Landau damping prohibits the occurrence of triggered RBS in plasmas at densities less than subquarter-critical density, when the electron temperatures are high. However, as mentioned in [172,173], FRS of the seed can still obstruct Brillouin amplification. The resonant conditions for the FRS of the seed are: $\omega_{seed} = \omega_{plasma} + \omega_{scattered}$ and $k_{seed} = k_{plasma} + k_{scattered}$, causing the scattered light to be downshifted from the seed by the plasma frequency [172]. The difference between the seed and the dispersed light must now be k_{plasma} because the seed and the scattered light copropagate [173,174] with a phase velocity, c in FRS, and the plasma wave is not easily Landau-damped.

$$k_{plasma} = \frac{\omega_{pump}}{c}\left[1 - \left(1 - \frac{\omega_e}{\omega_{pump}}\right)\right] = \frac{\omega_e}{c} \tag{13}$$

The growth rate of FRS (Γ_{FRS}), is evaluated by using the equation [173,174]

$$\Gamma_{FRS} = \frac{b_0}{2\sqrt{2}} \frac{\omega_e^2}{\omega_{pump}}, \tag{14}$$

where $b_0 = E_{0,seed}/E_{rel}$ is the normalised seed amplitude. Here, $E_{0,seed}$ is the maximum electric field of seed pulse and $E_{rel} = m_e\omega_L c/e$, is a constant. Equation (14) determines the growth rate of FRS, providing information about its effect on SBS. Because the growth rate of FRS is lower than that of SBS at a fixed a_0 and under typical conditions, the FRS of the pump should not be a major concern [168]. However, when the ratio of electric field strength of the seed (b_0) to that of the pump (a_0) equals the growth rate of Brillouin backscattering, FRS must be considered, i.e., the condition where $\Gamma_{FRS} = \Gamma_{SBS}$. To express this analytically in the strongly coupled regime, consider the equation below [168],

$$\omega = \left(\frac{1}{2} + i\frac{\sqrt{3}}{2}\right)\left[\frac{v_{osc}^2 k_{pump}^2 \omega_{pi}^2}{2\omega_{pump}}\right]^{\frac{1}{3}}, \tag{15}$$

where, $v_{osc} = a_0 c$ is the electron oscillation velocity and ω_{pi} is the ion plasma frequency. From Equations (14) and (15) and considering the constants, $2^{\frac{1}{6}}\, 3^{\frac{1}{2}} \approx 1.94$, the ratio $\frac{b_0}{a_0}$ can be written as

$$\frac{b_0}{a_0} = 1.94\left(\frac{Zm_e}{m_i}\right)^{\frac{1}{3}} \frac{1}{a_0^{\frac{1}{3}} N^{\frac{2}{3}}}. \tag{16}$$

Thus, the highest attainable seed intensity before FRS adversely affects the seed growth is approximated by the ratio b_0/a_0 for which $\Gamma_{FRS} = \Gamma_{SBS}$ [168]. For $\frac{n_0}{n_{cr}} > 0.05$, b_0/a_0 is less than 3, implying that it would not be feasible to amplify a seed to an intensity greater than 10 times that of the pump for $0.05 \leq N \leq 0.25$, where N is n_0/n_{cr}, for Brillouin amplification. Hence, the usefulness of SBS in this domain is severely constrained because the aim of parametric plasma amplification is to produce pulses of higher intensity than what can be produced in conventional solid-state systems. It should be emphasised here that FRS does not provide a challenge for $N > 0.25$, like RBS. The growth of FRS is slower than RBS and amplification by SRS typically takes place at lower plasma densities than amplification by SBS. Therefore, FRS does not have the same negative effects on Raman amplification as it does in the case of Brillouin amplification. It is worth noting here that when $\Gamma_{RBS} = \Gamma_{FRS}$, then we have

$$\frac{b_0}{a_0} = \frac{\sqrt{2}}{N^{3/4}}, \tag{17}$$

which has a minimum value of 4 at $N = 0.25$ and tends to increase to 45 at $N = 0.01$, which implies that the seed can be amplified to an intensity greater than 10 times that of pump.

3.2.2. Filamentation

Filamentation is yet another phenomena that needs to be addressed in order to get maximum amplification via the Brillouin amplification. Filamentation, or the transverse collapse of a laser beam caused by ponderomotive [175,176], relativistic [177,178], or thermal [179,180] changes in the refractive index of the plasma, can also limit the level of attainable amplification. An intensity-dependent change in the refractive index results in the self-focusing of a beam, which in turn causes filamentation. This occurs in plasmas due to heating, ponderomotive expulsion of electrons and ions, or a decrease in plasma frequency due to the relativistic increase in the mass of electrons in strong fields [168]. The challenge of filamentation instabilities at high plasma densities has been an important topic of research due to the usefulness of SBS at $N < 0.25$ [173,181].

3.3. Mitigating the Limiting Factors for Brillouin Amplification

Several factors define the regimes suitable for amplification of the seed pulse via Brillouin and Raman processes [71,161,181]. For example, the extent of amplification is constrained by the maximum duration of the pump pulse to prevent filamentation. The effectiveness of amplification needs to be high for the process to be useful. Therefore, there is a need to avoid wave breaking and a transition from weak coupling to strong coupling is advantageous. For Brillouin seed amplification, analysis of these factors initially led to the conclusion that plasma density should be suitably low because high density causes filamentation. In contrary to the strong coupling regime, very low density encourages weak coupling. Although long pulses may break, short pulses have inefficient energy transmission [126]. Despite the prominence of these considerations, several studies continued to concentrate on the range $n_0/n_{cr} > 0.25$ because the rate of Brillouin amplification in this regime is particularly high. Therefore, the primary goals of these investigations were to reduce wave breaking and filamentation. The following Section 3.3.1 will consider the progress made by using plasmas with densities less than subquarter-critical densities ($n_0/n_{cr} < 0.25$) for amplification and Section 3.3.2 briefs the investigations conducted in plasmas with densities above subquarter-critical densities ($n_0/n_{cr} > 0.25$).

3.3.1. Studies under Subquarter-Critical Plasma Densities

Plasma densities $\sim n_0/n_{cr} < 0.25$, notably in the range $0.05 < n_0/n_{cr} < 0.15$, have been the focus of majority of experimental research and numerical calculations [106,161,167,170,181]. In exchange for a lower growth of filamentation instability, these efforts accept the presence of parasitic SRS.

In a proof-of-concept experiment by E. Guillaume in 2014, the possibility of transmitting energy through stimulated Brillouin backscattering from a long pump pulse of 15 ps to a short seed pulse of 1 ps [161] was demonstrated, revealing the dependence of experimental parameters on Brillouin amplification and an optimal experimental condition for such experiments. This experimental observation of Brillouin scattering by using two beams from the same laser system shows that the transfer of energy to the Brillouin peaks and its wavelength depends on factors such as plasma density, intensity of laser pulses, two plasmon decay instability, and SRS instabilities. The experiments supported by OSIRIS (PIC code) revealed a substantial increase in the SBS signal with increasing plasma density [161]. These findings were reinforced by further studies [61] in which energy transfer from the pump to the seed of up to 2.5% has been obtained. The first experimental evidence of amplification of short pulses using sc-SBS in the pump depletion regime was reported in [61], where pulses of the same wavelengths were used. Here, energy transfer and amplification were demonstrated in the regime corresponding to SRS excitation. The decrease in amplification for densities higher than 0.1 n_c is correlated to the decreased transmission of the two pulses. In addition, these investigations reveal that lowering inhomogenities in the plasma density improves pulse propagation and attenuation. This happens because, in a homogeneous plasma, increasing plasma density above 0.25 n_c while maintaining low attenuation improves the interaction conditions leading to maximum amplification factor. Furthermore, the investigations also suggested that the effective interaction length could be increased by using a multistage configuration. Although these investigations [61,161] focused on increasing plasma density for mitigating the limitations of SBS for amplification, a group of other studies relied on optical chirp as a crucial strategy, in which the possibility of reducing SRS by manipulating pump/probe frequency chirp was explored [72]. The time evolution of a seed depended on the initial seed duration, in the linear nonchirped case. The spectrum featured two broad peaks (corresponding to the compression of the seed) which propagates outward from the center during the amplification process. The RBS of the pump caused by the thermal fluctuations in plasma is a significant problem that creates ultraintense, ultrashort laser pulses. A theoretical investigation of the RBS instability caused by plasma noise was reported in [182], explaining the effect of RBS in SBS. It was demonstrated that density gradients inside the plasma can be utilised to detune the Raman resonance such that it stabilises the backscatter of the pump from thermal noise while maintaining the functional Raman amplification of the seed [58]. Later, it was found that the pump was intrinsically chirped because the ps to ns long pulse was created by chirping a fs pulse that was collected from a CPA system [111]. Numerical PIC simulations in [183] showed that chirping of the pump decreases the undesirable effects in Brillouin amplification. A detailed investigation on the effect of optical chirp to Raman amplification [184] demonstrated the superradiant scaling in the linear domain of Raman seed development [185] triggering the investigation of the effect of chirping of the pump on the Brillouin amplification of the seed [72]. Here, the characteristics of the plasma and laser were selected to support the ion acoustic waves and hence, the interactions described were in the weak coupling regime [72]. The effect of the chirp rate on the seed profile and its amplification rate were discovered in this investigation, and it was also found that when this technique is used to maximise Brillouin seed amplification, the chirp should be powerful enough to prevent noticeable pump backscatter. Pulse width of the seed is another parameter that supports this aspect. Short pulses end up as relatively broader pulses following the initial redistribution in the linear regime, thereby demonstrating that broader starting pulses are preferable for plasma-based amplification. Experiments on sc-SBS amplification of a seed pulse by a chirped pump [166] demonstrated that chirping the pump has a strong influence on the shape of the seed in the nonlinear amplification regime, which could mitigate SRS of the pump before interacting with the seed. This experiment suggested that plasma densities lower than n_c avoid filamentation, and chirping the pump helps to lower parasitic effects in sc-SBS. The rate of amplification in the nonlinear regime, seed profile, and the linear seed development were influenced by chirp rate. An analytical model for unstable seed evolution using a chirped pump developed in this investigation proved that the evolution of the seed is not symmetric to the direction of the chirp. Compared to chirpless strong coupling, chirp lowers the exponential growth of FRS. However, in the nonlinear phase, the sign of the chirp affects the superradiant pulse shape. Choosing the right chirp can reduce tail oscillations and for the opposite chirp, Raman-like oscillations develop, affecting the maximum attainable amplitude of the seed. The effect of chirping on various parameters are given in Figure 3.

A detailed analysis of the various stages in the strong coupling Brillouin plasma amplification, emphasising the importance of the chirp was investigated in [69]. This was found to be intrinsic to the amplification process, induced by chirped laser pulses, or connected with the plasma profile. Chirping could alter energy transmission, and the direction of energy flow is explained by the time-dependent phase relation [186]. Optimization of interaction conditions for efficient short laser pulse amplification by SBS in the strongly coupled regime was demonstrated in 2016 [186], supported by 1D PIC simulations with SMILEI, implying both the full kinetic treatment and all competing effects, such as spontaneous SBS, SRS, and FRS. It was observed here that amplification of short seed is possible depending on the intensity of the seed, and the amplification mechanism was found to differ for low and high intensity seed pulses. The seed may stretch before reaching a self-similar regime when the intensity is low, and at high intensities, if the matching condition for SRS is not satisfied, electron contribution becomes significant. It was also proven that it is challenging both experimentally as well as theoretically to amplify from low to high intensities in a single pass, and hence, a multistage process should be considered to provide large amplifications. In this process, the pulse amplified by a pump in a plasma cell should interact with another pump in the adjacent cell. However, in this case, issues related to self-focusing and filamentation become important owing to amplification of the seed pulse to relativistic intensities in this process. Similar work on nonlinear Brillouin amplification of finite-duration seed pulses in the strong coupling regime showed some qualitative similarities between Raman and sc-Brillouin seed growth [66], recommending the inclusion of spatial inhomogeneity, wave-particle interaction, and frequency chirping for the growth of seed pulses. In addition, it was suggested that precise limits caused by wave breaking and filamentation should be determined for effective amplification via parametric processes. Following this, most of the further investigations focused on the strong coupling regime for amplification of laser pulses.

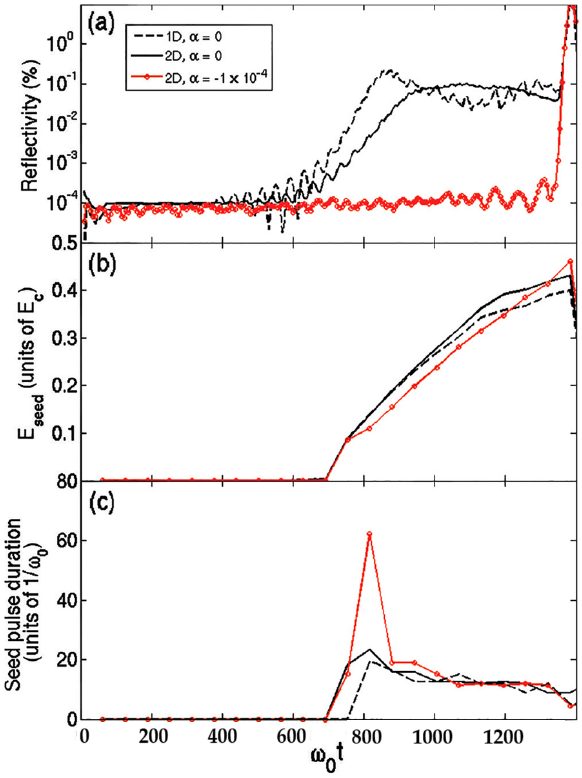

Figure 3. Temporal evolution of (**a**) the reflectivity, (**b**) the seed amplitude, and (**c**) the seed duration for unchirped and chirped pump laser beams in 1D and 2D geometries. The duration and the energy of the seed laser beam have been set equal to zero for time earlier than $\omega_0 t = 711$ (time at which the seed beam enters the plasma). Here, ω_0 is the frequency of the pump (given as ω_{pump} in the text). For the 2D geometry, the diagnostics were computed on axis. This figure was reprinted/adapted with permission from Ref. [183]. Copyright year: 2022, Publisher: American Physical Society.

Plasma-based laser amplification was considered as a possible way to overcome the technological limits of present-day laser systems to achieve exawatt laser pulses [55]. The first observation of the signatures of transition from linear to self-similar regimes of sc-SBS was reported here, where sub-ps pulses were amplified by a factor of 5 with an energy transfer of the order of a few tens of millijoules. Pulse shortening, spectral broadening, and downshifting were observed when the sc-SBS amplification entered the self-similar zone, thereby increasing the gain. This observation was further supported by the power law relationship between gain and amplification length; i.e., when the interaction length is doubled, the gain in energy and intensity increase by a factor of 1.4. An independent investigation on the impact of filamentation (caused by the relativistic self-focusing effect) in the amplification of short pulses by sc-SBS [169] found out that the filamentation instability destroys the amplified seed profile in sc-SBS amplification within a typical parameter area. Despite the fact that an increase in plasma density accelerates the formation of the sc-SBS, preventing Raman scattering, the filamentation instability adversely affects SBS. Although some previous reports suggested a nominal plasma density, $n_e/n_{cr} = 0.3$ [167] to eliminate Raman scattering in the sc-SBS, the high plasma density leads to severe filamentation instability, hindering effective amplification. The independent investigation on sc-SBS in [181,187] suggested a plasma density of $n_e/n_{cr} = 0.05$ to prevent filamentation. It was found that structured plasmas can exploit the effective energy transfer between a long pump pulse with high energy and a short seed pulse with low energy. Alongside this research, the spectra of ultrashort laser pulses in plasma amplifiers were investigated [187], supporting the claim in [181]. These investigations suggested that the amplification of laser pulses by plasmas are based on a coupling of three waves: two transverse electromagnetic waves and a longitudinal plasma response and that the SRS and SBS signals have been observed simultaneously. However, it was also found that the SRS and SBS signatures do not overlap. Kinetic simulations demonstrate that a pure sc-SBS amplification regime cannot be maintained for short seed pulses (10 fs) with high intensities ($\sim 10^{18}$ W/cm^2). The SRS or SBS processes were quenched when the plasma density exceeds $n_0/n_{cr} > 0.25$, making Raman excitation impossible, or if the frequency spread of the seed pulse ($\Delta\omega_s$) is inadequate to link with the initial SRS excitation, i.e., $\Delta\omega_s < \Delta\Omega \approx \omega_{pump} - \omega_{ep}$, before wave breaking. As densities below quarter-critical are more favourable [181] and extremely short pulses reach relativistic intensities faster, mixing is unlikely to be avoided in experiments. Analysing the spatial and temporal spectra obtained from 1D PIC simulations in [98], it was, however, observed that only SRS is present at plasma densities less than 0.25, and SBS is not present in this regime, which is contrary to the observation reported in [181,187]. Effects of pulse and seed intensities to commence the process, optimal ion and electron temperatures, plasma length, density profile, and its variations on the parametric processes remain unresolved at this stage, leaving room for tuning different parameters to maximise efficiency and intensity in the sc-SBS regime.

To fill the gap, an investigation of the possibility of mitigating SRS by adding an external magnetic field was presented in [188], wherein the best results were obtained at a plasma density of $n_0/n_{cr} = 0.01$, by using lower pulse intensities of the order of 10^{15} W/cm^2. Results of the simulation showed that a significant improvement in the amplification and compression ratios can be obtained either by lowering the plasma density or the pump intensity. Other theoretical investigations [189] introduced an external static magnetic field longitudinal to the laser propagation direction to enhance the performance of amplification in the sc-SBS regime. The magnetic field was found to enhance the sc-SBS amplification due to faster sc-SBS growth rate and less collisional damping. However, the amplified component of the seed shifts from the first peak to the second peak and subsequently the third peak as the seed intensity increases and the amplification enters the relativistic electron nonlinearity domain and exhibits oscillatory behaviour. It was also found that by decreasing self-modulation instability (SMI), a reversed magnetic field aids to obtain a higher output intensity and a smoother output pulse profile. Combining these two elements, a double-pass approach to enhance amplification in the presence of a longitudinal magnetic field is suggested. A magnetic field should also suppress filamentation as it does in SMI because the growth rate of filamentation has the same factor as that of SMI in the presence of a magnetic field, but confirming that will require a more complex 3D simulation. It is also pointed out that the maximum output power limit imposed by filamentation may be circumvented by employing an external magnetic field. The simulation model, however, does not take into account the wave breaking, renormalized forward scattering, or any other nonlinear effects, as these effects could quantitatively alter the outcomes of our experiment. From these simulations, the seed durations were found to compress to $\sim$100 fs. This is because the reciprocal of the frequency of the ion acoustic quasimode is of the order of several hundred fs. A more precise computation technique will be required for future research in this direction.

Even though all these studies mentioned above in the strong coupling regime are extremely relevant, the investigation presented in [18] created a unified two-wave model that can analyse the intermediate transition phase, which is valid in both weak and strong coupling regimes. It was demonstrated here that a dynamic transition from weak to strong coupling is possible only as a result of the rising seed amplitude during amplification. Therefore, the pump intensity by itself does not necessarily reveal the regime in which the interaction occurs. Moreover, because the traditional strong coupling models does not consider nonlinear seed growth, weakly coupled amplified regions appear in the tail of the seed and natural intensity variations for experimentally significant pulses only partially reach the strong coupling threshold. Hence, the shape of the amplified seed pulse differs, and the efficiency is decreased. Additionally, every amplifier configuration eventually produces a density beat that identifies the presence of weak and strong coupling.

A unified treatment of weak and strong coupling regime is therefore necessary and is formulated in this research. An entirely new approach was introduced in [53], wherein the modification of the plasma density profile was considered to mitigate the limitations affecting amplification. Amplification of sub-ps pulses by laser-plasmas above the joule threshold promises a new technology for the next generation of ultrahigh-intensity lasers. The relevance of employing a seed pulse with a high-enough starting intensity to quickly enter the self-similar regime and achieve a highly efficient (20%) sub-ps energy transfer is demonstrated, and spontaneous BRA resulted in the loss of seed energy in this technique. However, using a pump beam with a larger focal spot or a tilted wave front can mitigate this tendency [173]. It was also found that the output seed energy, intensity, and quality were limited by the homogeneity and extent of the spatio-temporal interaction volume, which was limited by laser beam energy and quality. A plasma with a density ramp and a higher temperature could possibly decrease beam losses from spontaneous Raman scattering and collisional damping without compromising sc-SBS gain, which was supported by the previous claim that shorter seed pulse reduces these losses and is better suited to the self-similar regime, improving pulse compression [173,186,190]. By using a longer pump and plasma, greater homogeneous and hyper-Gaussian focus can increase energy transfer. Hopefully, more powerful lasers will allow these advancements and pave the path for the next phase, a seed intensity far higher than the pump.

A recent report on improving the performance of Brillouin amplification at subquarter-critical densities by reducing the effects of parasitic Raman scattering [191] as a distinctive approach to produce ps pulses with PW power. Here, control over parasitic instabilities that accompany amplification was found to preserve the quality of the amplified pulse. Ponderomotive filamentation becomes a major threat for plasma densities $> 0.25n_{cr}$, but its growth rate does not change with density. Therefore, previous studies [53,169] proposed to perform Brillouin scattering at densities below $0.25n_{cr}$. Reducing the plasma density definitely reduces filamentation but poses the threat of parasitic Raman scattering; however, here the growth rate of RBS increases and the growth rate of FRS decreases. Hence, it is clear that parasitic Raman scattering must be reduced to boost Brillouin amplification [191]. It was found that experiments must be conducted at densities for which FRS is either impossible (i.e., $n_0/n_{cr} > 0.25$) or insignificant (i.e., $n_0/n_{cr} \leq 0.01$) to optimize amplification via SBS. For $0.01 < n_0/n_{cr} < 0.25$, the RBS of the pump and the FRS of the probe increases, which creates more disadvantages compared to the advantage of reduced probe filamentation [173]. It was also found that a tailored plasma density profile (i.e., a ramp rather than a plateau) reduces Raman scattering at lower densities, and it is important that the highest plasma density should face the probe pulse to ensure the stimulation of Brillouin scattering during the early stages of laser-plasma interaction, when the intensity of probe is low. This also takes care of the FRS that occurs later when the probe intensity is higher. A detailed investigation of the tailored plasma profiles is therefore of utmost importance in this field, and hence stays as a future prospect of amplification using plasmas.

3.3.2. Studies above Subquarter-Critical Densities

Brillouin amplification experiments at or above subquarter-critical densities were suggested in the developmental stages of SBS-based amplification of laser pulses in plasmas because FRS is forbidden in this region, helping in effective amplification. However, further studies improved this notion and introduced the concept that plasmas with densities greater than subquarter-critical densities can also be utilized for SBS-based amplification. Research in this direction was based on one of the first realizations of a plasma-based amplifier, whereby a short laser pulse from a KrF laser was amplified by absorbing energy from a laser with longer pulse duration [192]. Here, the system acts as a pulse compressor as the energy is transferred from the pump to the seed. The working of this system involves mixing of two anti-parallel laser beams in plasma that is enclosed by a solenoidal magnetic field, where the electrostatic plasma wave and the seed pulse extracts energy from the pump pulse. Based on this device, a laser-plasma-based amplifier working on SBS or SRS at densities ≥ 0.25, and capable of amplifying shorter laser pulses ($\sim$100 ps), was envisioned in [41]. To realize this plasma amplifier, the driving mode of the system must have a frequency similar to that of an ion-acoustic or Langmuir wave. The investigations also revealed insight on the characteristics of ion-acoustic frequency, including high coupling rate between the two laser beams, decreased sensitivity to variations in plasma density and temperature, and higher overall efficiency [41]. These studies suggested the use of a two-dimensional magneto-hydrodynamic code to forecast the development of flat plasma density and temperature profiles for the proposed amplifier model. Other independent investigations were underway in parallel to the abovementioned research, which focused on details such as creating short pulses to use with the plasma-based amplifier [193,194]. A detailed literature review explained the beam coupling equations relevant to such plasma-based amplifiers [195]. Following this, a novel model of Brillouin-based plasma amplification that generates an amplified pulse of $\sim$5 fs and with an unfocused intensity of 6×10^{17} W/cm^2 was theoretically described [196]. Here, circularly polarised pump and seed pulses with Gaussian transverse profiles, both with intensities of 2.74×10^{16} W/cm^2, counter-propagating in a $0.3n_c$ plasma, were used in the 2D PIC simulations, demonstrating that the amplified seed maintains excellent beam characteristics because quick compression prevents filamentation.

In [196], the amplified seed first goes through sc-SBS amplification in this regime, and the additional pulse-compression mechanism arises from the interaction of plasma-introduced negative group delay dispersion (GDD) and electron relativistic nonlinearity generated self-phase modulation (SPM). Because the Brillouin-amplified pulse has a short duration and an intensity close to relativistic intensity, SPM and GDD are effective for amplification [196]. In addition, the amplified seed may be compressed to the single-cycle regime as a result of these effects and this pulse-compression method operates successfully in plasma densities just above quarter-critical density and pump intensities of ($\approx 10^{16}$ W/cm^2. Although the quick compression by sc-SBS as well as the interaction between SPM and GDD are both possible in this parameter range, it is observed that the Raman instability destroying the laser pulse is not allowed. While the pulse parameters, interactions, and other factors were discussed in many reports, a few other investigations shed light on the effect of collisions in the plasma on the amplification of laser pulses via SBS at plasma densities $> 0.3\ n_c$ [172], owing to their importance in future ultrahigh-intensity laser systems. The effect of collisional processes on the transfer of energy between the pump and seed laser pulses in SBS was investigated, wherein the standard three-wave Brillouin scattering process were dampened by collision effects for constant pump-to-probe ratios, preventing the pump laser from scattering before interacting with the seed pulse [172]. The effectiveness of SBS was found to increase, and the contrast of the resulting seed laser beam was also enhanced noticeably due to the effect of collisions. It was also pointed out that the impact of increasing the plasma ion temperature causes the ion acoustic waves connected to both the typical three-wave Brillouin scattering and the beat wave driven Brillouin scattering processes to be Landau-damped, reducing the onset and significant expansion of the instability. Similar theoretical investigations using a 1D PIC simulation showed efficient, strongly coupled Brillouin amplification at $n_0/n_{cr} = 0.3$, where SRS is forbidden [167]. Here, compression based on backward parametric amplification in liquids or gases are investigated, as they offer much higher damage thresholds. But the pulse duration is limited by the phonon period. The flexibility of SBS-based amplification by changing different parameters has been examined in detail, and it was found that the amplification is affected by the parameters of the seed pulse and the electron temperature (temperature ratio, i.e., ZT_e/T_i was kept constant) of the plasma. Amplification factors of 334 and 3300 (in relation to the initial seed intensity) were obtained when the intensity of the seed pulse was reduced to 10^{14} and 10^{13} W/cm^2, respectively. These investigations suggested that the SBS response time can be reduced by switching to the sc-SBS regime and these SBS-based amplifiers can have a length of up to 10 linear gain lengths, depending on the noise level of the density. However, the model failed to capture the interaction with the ponderomotive filamentation instability (which forms transverse to the propagation direction) at such high densities, which poses a major disadvantage to the realization of the plasma-based amplifiers. A proper strategy to mitigate the filamentation process was put forth in [170], in which a robust SBS-based plasma amplifier at high plasma densities ($n_0/n_{cr} > 0.25$ was investigated by using analytical theory and multidimensional PIC simulation. A convenient density regime for efficient Brillouin amplification was identified, which gave compression ratios of 40, 60, and 72, and amplification ratios of 15, 30, and 40, for pump intensities of 10^{16} W/cm^2, 10^{15} W/cm^2 and 10^{14} W/cm^2, respectively. The increase in these ratios with decreasing pump intensity follows from the fact that the filamentation growth rate decays more rapidly with decreasing pulse intensity. In addition, using lower intensities calls for the employment of plasma columns. However, this might bring in further issues, such as a rise in the premature Brillouin backscattering of the pump before it encounters the probe, which can be avoided by adopting sophisticated pump focusing techniques, such as the flying focus [197], which avoids the propagation of the powerful pump through the plasma column before it encounters the probe. A similar investigation on Raman amplification with flying focus is given in Figure 4.

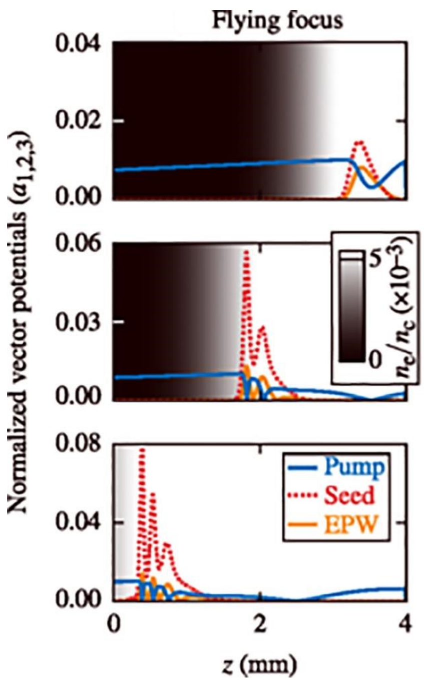

Figure 4. Results of simulations using a three-wave model. The pump first reaches a high intensity with the flying focus at the right edge, when ionisation is initiated. As various colours converge to various locations, constant intensity moves at $v = -c$, and as a result, the ionisation wave propagates at a nearly constant distance ahead of the injected seed pulse. We see the ideal plasma amplifier behaviour. This figure was reprinted/adapted with permission from Ref. [197]. Copyright year: 2022, Publisher: American Physical Society.

Mitigating speckle effects of the beam by using spike trains of uneven duration and delay pulses [198] could also be helpful for efficient amplification. Using large spot regions for the pump and seed pulses can lessen the divergence caused by speckles in the pump beam. Furthermore, a more uniform pump beam can be generated by employing strategies like random phase plates, smoothed spatial dispersion, or induced spatial incoherence [199], contributing to better amplification. However, these methods should be utilised with caution because they diminish the ability of the pump to generate SRS, SBS, and amplification in addition to flattening the envelope of the pump beam [65,200]. Further exploration of these non-ideal beam effects holds a future scope [170]. Another interesting investigation in this density regime to investigate the Brillouin scattering of a short seed laser pulse by a long pump laser pulse in a dense plasma, which employed the Eulerian

Vlasov code [201] to successfully solve the Vlasov–Maxwell set of 1D relativistic equations. Plasma density, $n_e/n_c = 0.3$ was used in these simulations to overcome amplification by SBS, and it was found that ion waves with a large amplitude were produced in these conditions. To understand these effects on the behaviour of the short input seed pulse, the duration and/or amplitude of the pulse was changed, and it was found that pulse broadening occurs more quickly for short pulses than long pulses. It was also observed that seed pulse with broad spectral span eventually becomes narrower and separates from the trailing signal as the simulation finishes. On the other hand, narrow seed pulses became broader. Because there is no noise in the Vlasov simulations, it is possible to model lengthy plasma amplifier, monitor the development of the system with a completely kinetic description, and accurately depict the distribution function phase-space structures.

It was evident from all the above investigations that a number of parameters, such as plasma density, seed pulse duration, intensity of seed pulse etc., affects Brillouin amplification at densities greater than 0.25 [145,170]. In addition to this, there are a few different parameters that affect Brillouin amplification directly or indirectly in this plasma density regime, as discussed below. The dependence of plasma temperature on Brillouin amplification was investigated, and it was found that there was no change in amplification with rising temperature near the front of the seed (around the seed maximum) as the density grating was not well developed there. However, as temperature changes, the tail of the seed was found to be changed. Fewer oscillations of the envelope of $\mid E_{\perp} \mid$ were seen at higher temperatures. It was also discovered in [202] that the density does not vary as much at the highest temperatures as it does at the lowest temperatures, and the wavelength of the envelope oscillations at the back of the seed is essentially constant for high temperatures. It was also verified that the maximum density perturbation in the range of density grating regime scaled is at $1/\sqrt{T_e}$ [201].

Another group of researchers focused on investigating the effects of pump intensity on Brillouin amplification through simulations and analytical theory [203]. Even though Brillouin scattering is not the best option for producing ultrashort, ultraintense pulses because of its lower growth rate and maximum pump-to-probe compression ratio when compared to the Raman amplification, it is more tolerant of the pump, probe, and plasma frequency mismatches, and therefore it can be the best possible candidate to compress pump beams of $\sim$0.1–1 ns [203]. However, it demands long plasma columns for this process and it may be difficult to maintain consistent plasma density and temperature along the entire column, which is again less crucial for Brillouin amplification than for Raman amplification. Lower pump intensity leads to a longer final probe according to the self-similar hypothesis of Brillouin amplification [203]. To move from the linear regime to the pump depletion regime, the initial probe duration must increase with decreasing initial probe intensity. According to the findings in [203], this is crucial as increasing spot size reduces pump and probe intensities. As the growth rate of Brillouin scattering is lower than Raman scattering, this affects Brillouin amplification more than Raman amplification. It was also found that filamentation restricts amplification more than ion-wave breaking, but it can be postponed with lower pump intensities. Maximum pump pulse duration, final probe pulse duration and intensity, and compression ratio scale, all improve pump intensity. The best pump-to-probe intensity amplification so far is 75, which might be 100–200 for lower pump intensities. The Brillouin scheme's durability offers promise for compressing lengthy (ns) beams to 10–20 ps duration. These findings may be corroborated by an earlier report, in which a two-stage Brillouin–Raman amplification technique was designed by using a Brillouin amplifier [59,204]. This technique combines the advantages of both SBS and SRS to amplify short laser pulses. The first stage requires a large plasma volume due to the large spot diameter and duration of the input pump beam, but Brillouin amplification can handle that; the second stage only requires a small plasma volume, so Raman amplification becomes practical, and Raman amplification provides the high compression ratios and short pulse durations.

Similar research around the globe supported the idea of employing laser plasmas for amplification due to their ability to handle high intensities without worrying about the damage thresholds as in solid-state media. Investigations on amplification of short pulses in the sc-SBS regime revealed that there are a number of regimes and applications for which plasma-based Brillouin amplification is both an interesting and promising route towards the generation of high-intensity lasers, as this regime allows shorter pulse durations, and may be suitable for amplification of ps and sub-ps pulses [205]. Investigations also suggest that sc-SBS offers a promising alternative to SRS for plasma-based amplification. However, optimizing conditions under which sc-SBS amplifiers excel requires further study. One such research reported a highly efficient Brillouin amplification of a strong Stokes seed providing an output energy of ∼400 mJ and an augmented efficiency of roughly 85% when the energies of the Stokes beam and pump beam are in the ratio of 39.5/1 [206].

Brillouin amplification has traditionally been used to boost weak seed signals or achieve high amplification gains [207,208]. For instance, reports of amplification of 300 times when the signal was 2.5 μJ and the pump was 6.5 mJ [209], 2×10^9 times when the signal was 10^{-11} J of Stokes beam [207] are available in the literature. Furthermore, other studies investigated the effect of amplifying a weak Stokes signal from SBS by a factor of more than two [208]. Finding the theoretical modelling in [206] indicates that the Brillouin medium's high gain and low absorption contribute to the output laser's high energy and power. When the energy of the Stokes beam (E_s) is high, the interaction length should be set to a lower value to minimise the impact of absorption.

4. A Comparison of Raman and Brillouin Scattering

As discussed in Section 1, plasma amplifiers are of great importance in the production of ultrahigh intensity, ultrashort laser pulses because they have a larger damage threshold over the well-developed solid-state systems [126]. Practically, an appropriate system capable of laser amplification should be reliable, strong, and reasonably adaptable in terms of frequency, intensity, duration, and polarisation. Moreover, it is challenging to create a big, totally uniform plasma; hence, the amplification mechanism must be somewhat resistant to temperature or density inhomogeneities. As mentioned in Sections 2 and 3, popular choices in this regard are SRS and SBS. Both have their own benefits and limitations, which are discussed in this section and a comparison is presented in Table 1.

For instance, the benefits of Brillouin amplification over Raman amplification have been listed as follows. (1) The frequency of the pump and seed lasers may be nearly identical and therefore the same laser can be used for both pump and seed [51,55,66,167,187,201]. (2) Energy loss to the plasma wave, modelled by the Manley–Rowe relations, may be lower for SBS than for SRS, which implies that more pump depletion can be attained [161,167,187]. (3) SBS is more resistant to plasma inhomogeneities in density or temperature than SRS [51,167,187]. (4) SBS is more suited for producing pulses with high total power or energy, in part because the use of larger-diameter plasmas allows for a lower sensitivity to inhomogeneity [173]. (5) In the regime $0.25 < N < 1$, only SBS occurs and Raman amplification does not happen [161]. (6) The duration of the Raman-compressed pulse may be compressed to within an order of magnitude of the Brillouin-amplified pulse, demonstrating that the two approaches are equivalent in terms of pulse compression [167]. (7) Because energy transmission is quick, a shorter contact length of plasma wave and seed pulse is needed for SBS, which is frequently measured for SRS as requiring ∼ mm to cm size plasmas whereas SBS can be achieved in 100 μm [167,181,201]. (8) In environments where SRS is constrained by particle trapping and wave breaking [155,210], SBS may be practical and can enable pump amplitudes that are many orders of magnitude larger than SRS. (9) SBS might be suitable in environments where collisional damping of Langmuir waves occurs [211].

Table 1. Comparison between Raman and Brillouin amplification.

	Raman Amplification	**Brillouin Amplification**
Frequency of pump and seed	Never identical	May or may not be identical
Energy loss to plasma wave	Comparatively low	Comparatively high
Plasma density ratio	Forbidden for density ratios > 0.25	Allowed in density ratios below and above 0.25
Contact length of plasma wave and seed pulse	Long	Short
Peak Intensities	Comparatively lower	Comparatively higher
Major Limitations	Forward Raman scattering, Langmuir wave breaking, super-luminous precursor of the amplified pulse, pulse scattering by plasma density inhomogeneties, parasitic effects of plasma noise on Raman scattering	Forward Raman Scattering, Filamentation

On the other hand, Raman amplification has the potential to produce higher peak intensities and amplification ratios [173,212], and the quicker plasma wave in timescale enables compression to experience shorter pulse durations. Although a better overall energy transfer between pump and seed has been attained with SBS, the experimentally demonstrated Raman amplifier surpasses Brillouin amplifiers in terms of energy-efficient transfer and peak intensity of the amplified seed [55,61]. In short, SBS offers superior conditions for amplification when compared to SRS due to its operational regime and lesser sensitivity to the factors mentioned above.

The current status of amplifiers based on SRS and SBS are presented in Figures 5 and 6. Figure 5 represents the intensities achieved via Raman amplification as a function of time since its development for time period from 2000 to 2022, along with the intensities predicted for Brillouin amplification. The majority of the investigations presented here indicate that the output intensities fall between 10^{15} and 10^{18} W/cm^2, with 10^{18} W/cm^2 being the highest output intensity achieved experimentally [213]. PIC simulations, on the other hand, produce an amplification of up to 10^{25} W/cm^2 [59].

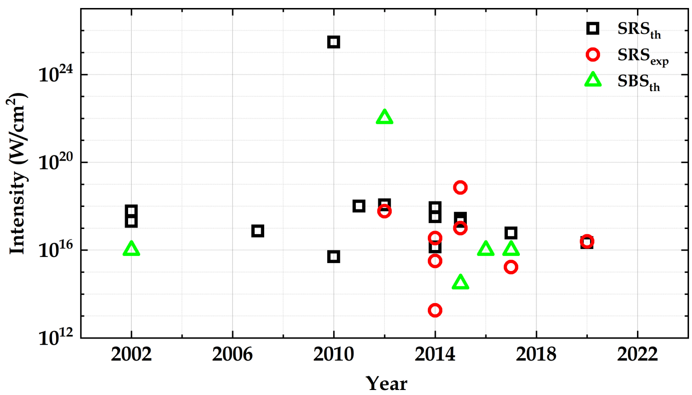

Figure 5. Intensity of the seed pulse predicted/obtained with time from 2000 to 2022 for Raman amplification and Brillouin amplification are presented here.

Figure 6 shows densities of the plasmas used in various investigations based on Raman amplification along with theoretical predictions on Brillouin amplification. Most of the research employs the density of the plasma in the range of 10^{17}–10^{22} cm^{-3} for both

Raman and Brillouin amplification. The highest value of density used in the experiments is 10^{22} cm^{-3} [213] and that in PIC simulations is 10^{25} cm^{-3} [214].

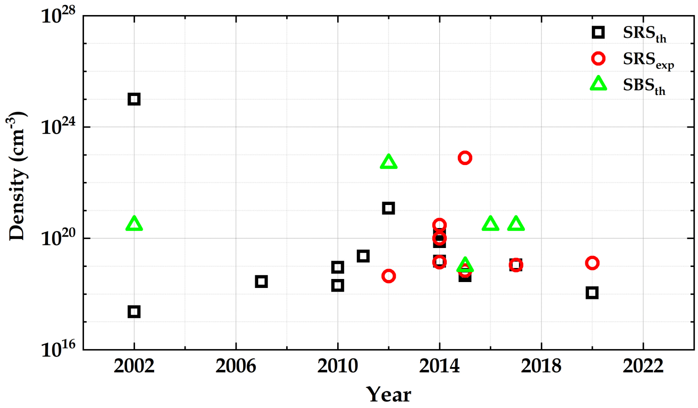

Figure 6. Density of the plasma predicted/obtained with time from 2000 to 2022 for Raman amplification and Brillouin amplification are presented here.

5. Amplification in Magnetized Plasma

SRS and SBS are the two established mechanisms for amplifying high-intensity laser pulses by using plasmas as the amplifying medium [29,55,60–62,66,68,69,98,106,123,126,137, 161,167,168,181,187,202,205,212,215–220]. Although SRS is mediated by Langmuir waves, SBS is mediated by ion-acoustic waves. However, there are drawbacks for both of these techniques. Although SRS provides a high growth rate but a large frequency shift, SBS provides high-efficiency energy extraction and less frequency separation but lower growth rate. A new scheme to overcome these disadvantages is implemented, in which a plasma with uniform density is substituted by a magnetized plasma, and the amplification process is mediated by ultrahybrid (UH) [221] or magneto-hydrodynamic (MHD) waves [222].

5.1. Theoretical Structure

To explain the amplification process, it is important to prove the dispersion relations in magnetized plasma and create a generalised three-wave interaction model for magnetic backward Raman amplification (MBRA) [223]. Toward this goal, an external magnetic field (B_0) in the y direction and wave propagation in the x direction (without average flows) in an isotropic Maxwellian plasma is considered. The equations for the electric field in such case can be written as [221]

$$\begin{pmatrix} \epsilon_{xx} & 0 & \epsilon_{xz} \\ 0 & \epsilon_{yy} - \frac{k^2c^2}{\omega^2} & 0 \\ \epsilon_{zx} & 0 & \epsilon_{zz} - \frac{k^2c^2}{\omega^2} \end{pmatrix} \begin{pmatrix} E_x \\ E_y \\ E_z \end{pmatrix} = 0, \tag{18}$$

and the components of the dielectric tensor are

$$\epsilon_{xx} = 1 - \frac{\omega_{plasma}^2}{\omega} \frac{e^{-\lambda}}{\lambda} \sum_{n=-\infty}^{\infty} \frac{n^2 I_n(\lambda)}{\omega - n\Omega} \tag{19}$$

$$\epsilon_{xz} = -\epsilon_{zx} = i\frac{\omega_{plasma}^2}{\omega} e^-\lambda \sum_{n=-\infty}^{\infty} \frac{n[I_n'(\lambda) - I_n(\lambda)}{\omega - n\Omega} \tag{20}$$

$$\epsilon_{yy} = 1 - \frac{\omega_{plasma}^2}{\omega} e^{-\lambda} \sum_{n=-\infty}^{\infty} \frac{I_n(\lambda)}{\omega - n\Omega} \tag{21}$$

$$\epsilon_{xx} = 1 - \frac{\omega_{plasma}^2}{\omega}\frac{e^{-\lambda}}{\lambda}\sum_{n=-\infty}^{\infty}\frac{[n^2 I_n(\lambda) + 2\lambda^2 I_n(\lambda) - 2\lambda^2 I_n'(\lambda)]}{\omega - n\Omega}, \tag{22}$$

where $\lambda = \frac{k^2\rho_e^2}{2}$ and $\rho_e = \frac{v_{te}}{\Omega}$ is known as the Larmor radius, Ω is the electron cyclotron frequency, and ω_{plasma} is the plasma frequency. According to the field equation given in Equation (18), two orthogonal modes are possible: (1) ordinary wave (O) and (2) extraordinary wave (X). The electric field of the ordinary wave is parallel to B_0 and corresponds to $\epsilon_{yy} - k^2c^2/\omega^2 = 0$ and the extraordinary wave is plane-polarized in the direction of B_0, and it satisfies the condition [221]

$$det\begin{pmatrix} \epsilon_{xx} & \epsilon_{xz} \\ \epsilon_{zx} & \epsilon_{zz} - k^2c^2/\omega^2 \end{pmatrix} = 0. \tag{23}$$

The same polarization is an essential factor for the coupling of the pump and seed laser, i.e., both should be either on the X-mode or the O-mode. The cold fluid approximation applies well for the pump and seed here, because the plasma frequency is very small compared to the laser frequency [224]. According to the cold fluid approximation, the dispersion relations of O-mode is given by [224]:

$$c^2k^2/\omega^2 = 1 - \omega_{plasma}^2/\omega^2, \tag{24}$$

and for the X-mode as

$$c^2k^2/\omega^2 = RL/S, \tag{25}$$

where $RL = 1 - \omega_{plasma}^2/[\omega(\omega \pm \Omega)]$ and $S = R + L/2$. The dispersion relations in Equations (24) and (25) also satisfy the resonantly excited electron Bernstein waves (EBW) [225] and the dispersion relation for EBW in the electrostatic approximation is [221]

$$\epsilon_{xx} = 0. \tag{26}$$

The above dispersion relation is applicable close to the UH resonance in the limit $T_e \to 0$ and $\omega_{UH} = \sqrt{\omega_{plasma}^2 + \Omega^2}$. Under electrostatic approximation, general three-wave coupling process for MBRA can be explained by a set of equation for the EBW and laser pulse wave envelopes [226]. We have

$$(\partial_t + c_a\partial_x)a = \frac{\omega_{plasma}}{2}bf \tag{27}$$

$$(\partial_t - c_b\partial_x - i\frac{\omega_{plasma}^2}{8\omega_0}b^2)b = -\frac{\omega_{plasma}}{2}af* \tag{28}$$

$$\partial_t f = -\frac{\omega_0\omega_{plasma}}{2\omega_3}ab*, \tag{29}$$

where a is the amplitude of the pump, b is the amplitude of the seed pulse, $f = eE_f/m_e\omega_{plasma}$ is the normalised amplitude of EBW, c_a is the group velocity of the pump, and c_b is the group velocity of seed, ω_3 is the frequency of excited EBW. The three-wave models for MBRA and backward Raman amplification (BRA) are similar, except for the coupling coefficient, which implies that the growth rate of both MBRA and BRA will be similar. The linear growth rate for MBRA is given by [221]

$$\Gamma_R = \frac{\sqrt{\omega_3\omega_0}}{2}|a_0|/\gamma_B, \tag{30}$$

where $\gamma_B = \omega_3/\omega_{plasma}$ is the magnetization factor, and a_0 is the initial normalised pump amplitude.

5.2. Laser Amplification in Strongly Magnetized Plasma

A detailed study about the backscattering of laser pulses in strongly magnetised plasma, mediated by magneto-hydrodynamic waves referred this scattering as magnetic low frequency (MLF) scattering, because it does not have an analogue in unionised media, and this backscattering disappears in a nonmagnetised plasma. MLF scattering is more efficient in amplification because the growth rate is larger than the Raman scattering, the frequency difference between the seed and and pump beams is small (offers a great engineering advantage), the bandwidth interaction is wide (which can be used for the generation of ultrashort pulses), and large group velocity dispersion helps in the compression of broad bandwidth amplified pulse to ultrashort time duration [188]. The MLF instability can be calculated by using the two-fluid model [227]. PIC simulations for a counter-propagating pump-seed geometry are used to check if the MLF instability is useful for the amplification of laser pulses [188]. In each case, the plasma density (N = 0.01), plasma length (L = 175 µm), and pump amplitude (a_0 = 0.007) were the same. The initial seed pulse has a pulse duration of 400 fs and both the seed and the pump are elliptically polarised with Stokes parameters Q = 0.78I_0, U = 0.49I_0, V = 0.38I_0 for the propagation through magnetized plasma and linearly polarized in the nonmagnetized case. From Figure 7, we can say that in comparison with SRS and SBS, MLF scattering exhibits a much larger growth rate and broader spectral response [188]. The simulations show that high-power, few-cycle pulses can be generated with relatively short plasma length so that the seed and pump can be prepared from the same source, which is considered as a great engineering advantage. The broad bandwidth of MLF scattering shown in the Figure 8, supports the amplification of ultrashort pulses. The broad bandwidth results from the fact that each individual MHD wave produces a large growth rate and also the MLF scattering contains multiple MHD waves.

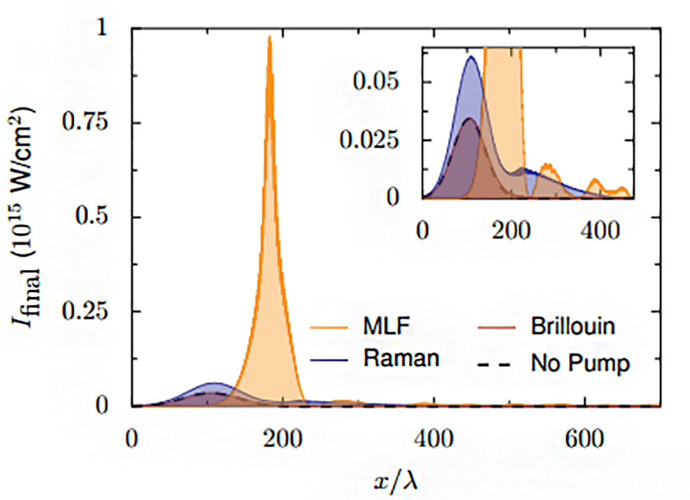

Figure 7. Final amplified seed after interaction in a plasma with N = 0.01, L = 175 λ) with a counter-propagating pump (a_0 = 0.007, λ = 1 µm, and $I = 6.7 \times 10^{13}$ W/cm^2. This figure was reprinted/adapted with permission from Ref. [188]. Copyright year: 2022, Publisher: American Physical Society.

A laser will be strongly backscattered from kinetic MHD waves when it propagates in a plasma at an oblique angle to a sufficiently strong magnetic field and this backscattering can be used for laser amplification [188]. In addition, substantial spectral broadening is observed in PIC simulations, supporting amplified pulses with ultrashort duration [188].

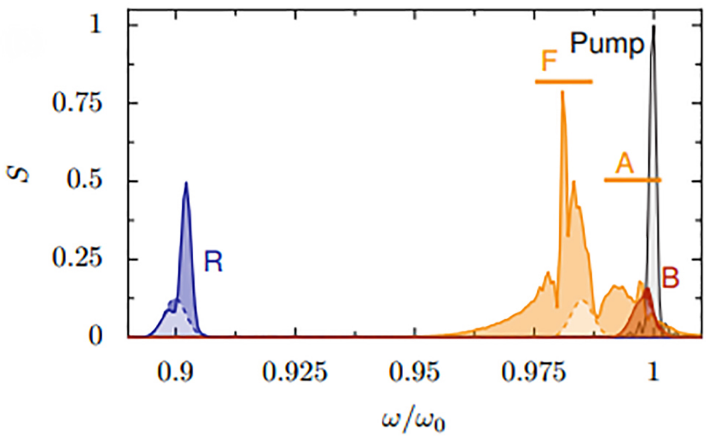

Figure 8. Spectra of the initial (dashed line) and amplified (solid line) seed pulses for SRS (R), SBS (B) and MLF (P,A), together with the pump spectrum. This figure was reprinted/adapted with permission from Ref. [188]. Copyright year: 2022, Publisher: American Physical Society.

5.3. Laser Pulse Compression Using Magnetised Plasma

Independent research found that the required plasma density can be reduced by an external magnetic field transverse to the direction of propagation [226]. In pulse compression mediated by magnetised plasma and the parametric interactions reduces the wave damping and instabilities, enabling the pumps, which are of higher frequency or lower intensity to produce pulses at higher intensities and longer duration. In addition to that, the method established in the research minimizes the need for high-density uniform plasmas. The advantage of using the transverse magnetic field is realized by evaluating the pulse compression mediated by UH waves, which can compress the high-power laser pulses beyond the current abilities and also at lower frequencies [226]. It is found that the solutions of unmagnetized and magnetised cases are comparable, but the processes that limit pulse compression are different, which is very important and leads to different constraints on the pulse amplification regimes. The main limiting factors that affect the pulse compression are wave breaking, modulational instability with growth rate, collisionless damping of the UH wave and collisional damping of both the laser and the UH wave [40,51,54]. Pulse compression using unmagnetized plasma is not efficient. However, applying a magnetic field of the order of gigagauss by using hydrogen plasma can increase its efficiency [71]. The application of a strong magnetic field reduces the necessary plasma density, which will in turn reduce wave damping, making it possible to compress the pulse to ultrashort regimes (from ps to fs). According to an investigation, to compress a 500 fs pulse a plasma length of only 0.3 mm is required.

In conclusion, the method mentioned above enables the compression of high-power lasers by substituting high plasma density with magnetised plasma and the mediating wave is a UH wave rather than a Langmuir wave. Detrimental effects caused due to high density plasma are reduced, and the method eases out the engineering requirements of producing and maintaining high and uniform plasma densities.This method enables higher-frequency, lower-intensity pumps to produce pulses of both higher intensity and longer duration.

5.4. Amplification of Mid-Infrared Lasers via Magnetized Plasma Coupling

The analytical formula for the backscattering growth rate in a magnetised plasma by matching the three-wave resonance conditions numerically was simulated to theoretically prove the conditions enabling amplification of mid-infrared lasers via magnetized plasma coupling [228]. Plasma amplifiers provide resonance via the collective modes in already ionised media. Although the Langmuir wave and the acoustic wave mediated the Raman and Brillouin scattering in an unmagnetised plasma, the UH waves and the kinetic and magneto-hydrodynamic waves are responsible for these processes in the case of a magnetised plasma [188]. Laser-plasma coupling in a magnetised plasma heavily depends up on the laser polarization [228]. When $\Omega \approx c_s k_3$, magnetisation starts to affect the Brillouin scattering, when $\Omega \approx \omega_{plasma}$, the Raman scattering is affected and when $\Omega \approx \omega_{pump}$, the laser-plasma coupling is drastically enhanced [228]. When the participating waves have mixed characteristics, the coupling is stronger and the coupling weakens when the degree of hybridization (i.e., where different branches of UH wave cross and hybridize) is reduced because the mediating mode with stronger cyclotron character gives weaker coupling. When the laser polarization is aligned well with electron cyclotron motion, the coupling is stronger because electron-dominated modes provide larger coupling than ion-dominated modes. From the results of some research considering amplification of mid-infrared lasers in the range $\Omega_e/\omega_{pump} \approx 0.1$, the maximum pump intensity (limited by the wave breaking) was found to be 10^{12} W/cm^3. The maximum amplification time, limited by the modulational instability, was found to be $\sim$102 ps and the corresponding length of the mediating plasma was found to be $\sim$1 cm. This system provided an output pulse with an unfocused intensity of $\sim 10^{15}$ W/cm^2 and a pulse duration of $\sim$1 ps, after the nonlinear pulse compression. It was observed that the growth rate differs considerably for Raman and Brillouin processes, when the magnetic fields become nonnegligible, and the growth rate depends sensitively on the laser polarization.

5.5. Kinetic Simulations of Laser Parametric Amplification in Magnetized Plasmas

In addition to the abovementioned investigations, PIC simulations using the MBRA formula verified that parametric amplification in plasmas can be enhanced by replacing the uniform density plasma with a magnetized plasma, where the magnetic field applied is of the order of few megagauss. Simulations using a linearly polarized pump laser, with wavelength of 1 µm and a constant intensity profile and a temporal Gaussian seed pulse with polarization similar to that of the pump and with the central frequency of 0.905 ω_0 were conducted to investigate the laser parametric amplification in magnetized plasmas. Electron temperature was initialised at 40 eV, and an external magnetic field was applied perpendicularly to the pump and seed pulse. Assuming 100 electrons per cell, 80 cells per laser wavelength, and 85 time steps per laser period provides the resolution for the simulations. Two kinetic effects were demonstrated in the simulation, namely the wakefield generation (i.e., the process in which the energy of amplified pulse is depleted) and phase mixing (which destroys the coherence of the plasma wave). The more the magnetisation factor, the larger the electromagnetic component in the wakefield, causing depletion in the energy of the amplified pulse. The results of this simulation establish that magnetized resonance remains coherent even if the pump amplitude is more than wave-breaking threshold. Because of this, large intensity pumps in magnetized plasma will get greater output intensity than expected.

5.6. Laser-Plasma Interactions in Magnetized Environment

Investigations into the various laser-plasma interactions in a magnetized environment provided an insight to the processes responsible for Raman and Brillouin amplification processes [229]. Processes such as coherent scattering of lasers, laser pulse compression, and laser propagation and their effects on pulse compression in a magnetized environment are addressed in detail in these investigations. Owing to the benefits of applying magnetic fields in laser compression, the engineering challenge in producing high-density plasma was solved. In addition, applying a magnetic field reduces wave damping and stifles competing instabilities [40,51,54]. This allows us to use a magnetic field as an extra control variable, for increasing the efficiency of laser compression. Moreover, the compression of soft X-ray pulses, which was not possible in nonmagnetized cases is now possible with upper hybrid mediation. The results of such simulations must be verified by more complex simulations and experiments, and the possibilities of using other mediating waves like Alfven waves, hybrid waves, and Bernstein waves in magnetised plasma must be explored [223].

6. Conclusions

In conclusion, the SRS and SBS processes are compared in view of applying stimulated scattering techniques for amplifying high-energy laser pulses. The regimes that are best for amplification of the seed pulse by Brillouin and Raman processes are analysed by carefully choosing a number of variables, such as plasma density, maximum duration of pump pulse, intensity of pump pulse, etc. There are many potential limitations with Raman or Brillouin amplification techniques. In both cases, the priority is to prevent spontaneous RBS of the pump pulse due to random density variations. Moreover, in Raman schemes, it is necessary to prevent the plasma wave from breaking in order to maintain the rate of energy transmission. However, particle trapping will begin to take place even before the wave breaks, which will cause a reduction in the efficiency of amplification. At higher plasma densities in particular, when filamentation of the pulses can happen in conjunction with large seed amplitudes, Brillouin amplification is likely to be used. Spontaneous backscatter, wave-breaking, and filamentation are only a few factors that restrict the range of possible parameter values for amplification. Additional limits are imposed by experimental factors such as plasma temperature, density, amplitude, and duration of the seed. Hence, several simulation studies were carried out to optimize the different parameters for both schemes.

High amplification is expected in Raman and Brillouin scattering. However, the theoretical ideas were not widely realized experimentally. Even though Raman and Brillouin amplification in plasma were found beneficial to attain multiple PW powers, no plasma-based Raman amplification beyond 0.1 TW have been reported, and there are only very few reports on Brillouin amplification leading to powers of up to 1 TW. The initial seed duration and amplification should be chosen carefully, as it can delay the amplification of seed pulse and in turn, reduce the efficiency. All experiments conducted to date fail to achieve the necessary conditions for efficient amplification. Experimental realization with a significant (>10%) energy transfer from the pump to a short amplified seed pulse was observed only in few experiments (e.g., [53]).

A novel approach to address these drawbacks is to replace the plasma with uniform density with a magnetised plasma, and using ultrahybrid or magneto-hydrodynamic waves to mediate the amplification process. Plasma is capable of serving not only as a medium for amplification, but also as a medium for manipulating highly intense laser pulses. Recent years have seen the emergence of a new field of optics known as plasma-based optics, which examines the use of spatially organised plasmas as optical devices. Plasmas can also serve as polarizers and Bragg mirrors for ultrashort and ultraintense laser pulses. However, the capacities of plasmas for these applications are not yet understood, and hence they have immense potential for the application of plasma-based optics in the development of high-power lasers, i.e., multi-PW lasers.

Author Contributions: Literature review, manuscript outline, writing and original draft preparation, R.M.C.; acquisition of materials, sub-topic relevant literature review and original draft preparation, N.V. and R.S.S.; writing, editing and validation, writing guidance, K.H.R. and N.S.; supervision, N.S. All authors have read and agreed to the published version of the manuscript.

Funding: This research received no external funding.

Institutional Review Board Statement: Not applicable.

Informed Consent Statement: Not applicable.

Data Availability Statement: Not applicable.

Acknowledgments: Renju Miriam Cheriyan and Nikhil Varghese are thankful to the support provided by the Mahatma Gandhi University through the Fellowships for Research Students as part of promoting Research activities. All authors thank Achu Purushothaman for the fruitful discussions.

Conflicts of Interest: The authors declare no conflict of interest.

Abbreviations

The following abbreviations are used in this manuscript:

BRA	Backward Raman Amplification
CPA	Chirped Pulse Amplification
CPRA	Chirped Pulse Raman Amplification
CWB	Coherent Wave Breaking
EBW	Electron Bernstein Waves
FEL	Free Electron Lasers
FRS	Forward Raman Scattering
FWHM	Full Width at Half Maximum
GDD	Group Delay Dispersion
ICF	Inertial Confinement Fusion
ISI	Induced Spatial Incoherence
LWFA	Laser Wakefield Acceleration
MBRA	Magnetic Backward Raman Amplification
MHD	Magneto-hydrodynamic
MLF	Magnetic Low Frequency
OAM	Orbital Angular Momentum
PIC	Particle-in-cell
SBS	Stimulated Brillouin Scattering
SMI	Self Modulation Instability
SM-LWFA	Self-modulated Laser Wakefield Acceleration
SPM	Self Phase Modulation
SRA	Stimulated Raman Amplification
SRS	Stimulated Raman Scattering
SRSS	Stimulated Raman Side Scattering
sc-SBS	Strongly Coupled-Stimulated Brillouin Scattering
wc-SBS	Weakly Coupled-Stimulated Brillouin Scattering
RBS	Raman Backscattering
sc-SBS	Strongly Coupled-Stimulated Brillouin Scattering
wc-SBS	Weakly Coupled-Stimulated Brillouin Scattering
RBS	Raman Backscattering
UH	Ultra Hybrid

References

1. Maiman, T. Optical and microwave-optical experiments in ruby. *Phys. Rev. Lett.* **1960**, *4*, 564. [CrossRef]
2. Bloembergen, N. Nonlinear optics and spectroscopy. *Rev. Mod. Phys.* **1982**, *54*, 685. [CrossRef]
3. Sheehy, B.; DiMauro, L. Atomic and molecular dynamics in intense optical fields. *Annu. Rev. Phys. Chem.* **1996**, *47*, 463–494. [CrossRef]
4. Betti, R.; Hurricane, O. Inertial-confinement fusion with lasers. *Nat. Phys.* **2016**, *12*, 435–448. [CrossRef]
5. Keefe, D. Inertial confinement fusion. *Annu. Rev. Nucl. Part. Sci.* **1982**, *32*, 391–441. [CrossRef]
6. Craxton, R.; Anderson, K.; Boehly, T.; Goncharov, V.; Harding, D.; Knauer, J.; McCrory, R.; McKenty, P.; Meyerhofer, D.; Myatt, J.; et al. Direct-drive inertial confinement fusion: A review. *Phys. Plasmas* **2015**, *22*, 110501. [CrossRef]
7. Lianqiang, S.; Fengjuan, W.; Zongqiang, Y.; Weiwu, W.; Hongbo, C.; Chao, T.; Feng, Z.; Tiankui, Z.; Zhigang, D.; Wenshuai, Z.; et al. Research progress of kinetic effects in laser inertial confinement fusion. *High Power Laser Part. Beams* **2020**, *33*, 012004.
8. Gao, Y.; Cui, Y.; Ji, L.; Rao, D.; Zhao, X.; Li, F.; Liu, D.; Feng, W.; Xia, L.; Liu, J.; et al. Development of low-coherence high-power laser drivers for inertial confinement fusion. *Matter Radiat. Extrem.* **2020**, *5*, 065201. [CrossRef]
9. Wang, G. A brief review of the progress of laser inertial confinement fusion in recent years. *Chin. J. Nucl. Sci. Eng.* **1997**, *17*, 266–269.
10. Bingham, R.; Mendonca, J.; Shukla, P. Plasma based charged-particle accelerators. *Plasma Phys. Control. Fusion* **2003**, *46*, R1. [CrossRef]
11. Malka, V.; Faure, J.; Gauduel, Y.A.; Lefebvre, E.; Rousse, A.; Phuoc, K.T. Principles and applications of compact laser–plasma accelerators. *Nat. Phys.* **2008**, *4*, 447–453. [CrossRef]
12. Katsouleas, T. Progress on plasma accelerators: From the energy frontier to tabletops. *Plasma Phys. Control. Fusion* **2004**, *46*, B575. [CrossRef]

13. Bingham, R. Basic concepts in plasma accelerators. *Philos. Trans. R. Soc. A Math. Phys. Eng. Sci.* **2006**, *364*, 559–575. [CrossRef] [PubMed]
14. Esarey, E.; Schroeder, C.; Leemans, W. Physics of laser-driven plasma-based electron accelerators. *Rev. Mod. Phys.* **2009**, *81*, 1229. [CrossRef]
15. Downer, M.; Zgadzaj, R.; Debus, A.; Schramm, U.; Kaluza, M. Diagnostics for plasma-based electron accelerators. *Rev. Mod. Phys.* **2018**, *90*, 035002. [CrossRef]
16. Katsouleas, T. Plasma accelerators race to 10 GeV and beyond. *Phys. Plasmas* **2006**, *13*, 055503. [CrossRef]
17. Umstadter, D.P. All-laser-driven Thomson X-ray sources. *Contemp. Phys.* **2015**, *56*, 417–431. [CrossRef]
18. Schoenlein, R.; Elsaesser, T.; Holldack, K.; Huang, Z.; Kapteyn, H.; Murnane, M.; Woerner, M. Recent advances in ultrafast X-ray sources. *Philos. Trans. R. Soc. A* **2019**, *377*, 20180384. [CrossRef]
19. Corde, S.; Phuoc, K.T.; Lambert, G.; Fitour, R.; Malka, V.; Rousse, A.; Beck, A.; Lefebvre, E. Femtosecond X rays from laser-plasma accelerators. *Rev. Mod. Phys.* **2013**, *85*, 1. [CrossRef]
20. Wang, S.; Baumgarten, C.M.; Wang, Y.; Reagan, B.A.; Rockwood, A.P.; Wang, H.; Yin, L.; Wernsing, K.; Bravo, H.; Luther, B.M.; et al. High-power ultrashort pulse lasers to pump plasma-based soft X-ray lasers. *IEEE J. Sel. Top. Quantum Electron.* **2019**, *25*, 1–15. [CrossRef]
21. Albert, F.; Thomas, A.G. Applications of laser wakefield accelerator-based light sources. *Plasma Phys. Control. Fusion* **2016**, *58*, 103001. [CrossRef]
22. Liang, E. Gamma-ray and pair creation using ultra-intense lasers and astrophysical applications. *High Energy Density Phys.* **2013**, *9*, 425–427. [CrossRef]
23. Remington, B.A.; Drake, R.P.; Ryutov, D.D. Experimental astrophysics with high power lasers and Z pinches. *Rev. Mod. Phys.* **2006**, *78*, 755. [CrossRef]
24. Takabe, H.; Kuramitsu, Y. Recent progress of laboratory astrophysics with intense lasers. *High Power Laser Sci. Eng.* **2021**, *9*, e49 . [CrossRef]
25. Ditmire, T.; Edens, A.D. Laboratory simulations of astrophysical blast waves with high energy lasers. *Laser Photonics Rev.* **2008**, *2*, 400–416. [CrossRef]
26. Burns, F. High-power lasers their performance, limitations, and future. *IEEE Spectr.* **1967**, *4*, 115–120. [CrossRef]
27. Fork, R.; Shank, C.; Yen, R. Amplification of 70-fs optical pulses to gigawatt powers. *Appl. Phys. Lett.* **1982**, *41*, 223–225. [CrossRef]
28. Pogorelsky, I.V.; Fischer, J.; Kusche, K.; Babzien, M.; Kurnit, N.; Bigio, I.; Harrison, R.; Shimada, T. Subnanosecond multi-gigawatt CO/sub 2/laser. *IEEE J. Quantum Electron.* **1995**, *31*, 556–566. [CrossRef]
29. Malkin, V.; Shvets, G.; Fisch, N. Ultra-powerful compact amplifiers for short laser pulses. *Phys. Plasmas* **2000**, *7*, 2232–2240. [CrossRef]
30. Mourou, G.A.; Barty, C.; Perry, M.D. Ultrahigh-Intensity Laser: Physics of the Extreme on a Tabletop. USA, 1997. Available online: https://physicstoday.scitation.org/doi/10.1063/1.882131 (accessed on 9 November 2022).
31. Bahk, S.W.; Rousseau, P.; Planchon, T.; Chvykov, V.; Kalintchenko, G.; Maksimchuk, A.; Mourou, G.; Yanovsky, V. Generation and characterization of the highest laser intensities (10^{22} W/cm^2). *Opt. Lett.* **2004**, *29*, 2837–2839. [CrossRef]
32. Yu, T.J.; Lee, S.K.; Sung, J.H.; Yoon, J.W.; Jeong, T.M.; Lee, J. Generation of high-contrast, 30 fs, 1.5 PW laser pulses from chirped-pulse amplification Ti: Sapphire laser. *Opt. Express* **2012**, *20*, 10807–10815. [CrossRef] [PubMed]
33. Vaupel, A.; Bodnar, N.; Webb, B.; Shah, L.; Richardson, M.C. Concepts, performance review, and prospects of table-top, few-cycle optical parametric chirped-pulse amplification. *Opt. Eng.* **2013**, *53*, 051507. [CrossRef]
34. Tabak, M.; Hammer, J.; Glinsky, M.E.; Kruer, W.L.; Wilks, S.C.; Woodworth, J.; Campbell, E.M.; Perry, M.D.; Mason, R.J. Ignition and high gain with ultrapowerful lasers. *Phys. Plasmas* **1994**, *1*, 1626–1634. [CrossRef]
35. Lehmann, G. Plasma-Based Methods for Amplification and Manipulation of High-Power Laser Pulses. In *Proceedings of the NIC Symposium 2018*; No. FZJ-2018-02948; John von Neumann-Institut für Computing: Jülich, Germany, 2018
36. Seres, J.; Seres, E.; Hochhaus, D.; Ecker, B.; Zimmer, D.; Bagnoud, V.; Kuehl, T.; Spielmann, C. Laser-driven amplification of soft X-rays by parametric stimulated emission in neutral gases. *Nat. Phys.* **2010**, *6*, 455–461. [CrossRef]
37. Dai, J.; Xie, X.; Zhang, X.C. Terahertz wave amplification in gases with the excitation of femtosecond laser pulses. *Appl. Phys. Lett.* **2007**, *91*, 211102. [CrossRef]
38. Kuwahara, K.; Takahashi, E.; Matsumoto, Y.; Kato, S.; Owadano, Y. Short-pulse generation by saturated KrF laser amplification of a steep Stokes pulse produced by two-step stimulated Brillouin scattering. *JOSA B* **2000**, *17*, 1943–1947. [CrossRef]
39. Gorbunov, V.A.; Papernyĭ, S.; Petrov, V.; Startsev, V. Time compression of pulses in the course of stimulated Brillouin scattering in gases. *Sov. J. Quantum Electron.* **1983**, *13*, 900. [CrossRef]
40. Capjack, C.; James, C.; McMullin, J. Plasma KrF laser pulse compressor. *J. Appl. Phys.* **1982**, *53*, 4046–4053. [CrossRef]
41. Milroy, R.; Capjack, C.; James, C. A plasma-laser amplifier in the 11–16 μm wavelength range. *Plasma Phys.* **1977**, *19*, 989. [CrossRef]
42. Maier, M.; Kaiser, W.; Giordmaine, J. Intense light bursts in the stimulated Raman effect. *Phys. Rev. Lett.* **1966**, *17*, 1275. [CrossRef]
43. Gudzenko, L.I.; Shelepin, L.A.; Yakovlenko, S.I. Amplification in recombining plasmas (plasma lasers). *Sov. Phys. Uspekhi* **1975**, *17*, 848. [CrossRef]
44. Hora, H. Self-focusing of laser beams in a plasma by ponderomotive forces. *Z. Phys. A Hadron. Nucl.* **1969**, *226*, 156–159. [CrossRef]

45. Hora, H. Theory of relativistic self-focusing of laser radiation in plasmas. *JOSA* **1975**, *65*, 882–886. [CrossRef]
46. Esarey, E.; Sprangle, P.; Krall, J.; Ting, A. Self-focusing and guiding of short laser pulses in ionizing gases and plasmas. *IEEE J. Quantum Electron.* **1997**, *33*, 1879–1914. [CrossRef]
47. Sakai, O.; Tachibana, K. Plasmas as metamaterials: A review. *Plasma Sources Sci. Technol.* **2012**, *21*, 013001. [CrossRef]
48. Sakai, O.; Sakaguchi, T.; Tachibana, K. Verification of a plasma photonic crystal for microwaves of millimeter wavelength range using two-dimensional array of columnar microplasmas. *Appl. Phys. Lett.* **2005**, *87*, 241505. [CrossRef]
49. Lehmann, G.; Spatschek, K. Plasma-based polarizer and waveplate at large laser intensity. *Phys. Rev. E* **2018**, *97*, 063201. [CrossRef] [PubMed]
50. Forslund, D.; Kindel, J.; Lindman, E. Theory of stimulated scattering processes in laser-irradiated plasmas. *Phys. Fluids* **1975**, *18*, 1002–1016. [CrossRef]
51. Milroy, R.; Capjack, C.; James, C. Plasma laser pulse amplifier using induced Raman or Brillouin processes. *Phys. Fluids* **1979**, *22*, 1922–1931. [CrossRef]
52. Andreev, A.A.; Sutyagin, A. Feasibility of optical pulse compression by stimulated Brillouin scattering in a plasma. *Sov. J. Quantum Electron.* **1989**, *19*, 1579. [CrossRef]
53. Marquès, J.R.; Lancia, L.; Gangolf, T.; Blecher, M.; Bolaños, S.; Fuchs, J.; Willi, O.; Amiranoff, F.; Berger, R.; Chiaramello, M.; et al. Joule-level high-efficiency energy transfer to subpicosecond laser pulses by a plasma-based amplifier. *Phys. Rev. X* **2019**, *9*, 021008. [CrossRef]
54. Malkin, V.; Shvets, G.; Fisch, N. Fast compression of laser beams to highly overcritical powers. *Phys. Rev. Lett.* **1999**, *82*, 4448. [CrossRef]
55. Lancia, L.; Giribono, A.; Vassura, L.; Chiaramello, M.; Riconda, C.; Weber, S.; Castan, A.; Chatelain, A.; Frank, A.; Gangolf, T.; et al. Signatures of the self-similar regime of strongly coupled stimulated Brillouin scattering for efficient short laser pulse amplification. *Phys. Rev. Lett.* **2016**, *116*, 075001. [CrossRef] [PubMed]
56. Moody, J.; MacGowan, B.; Glenzer, S.; Kirkwood, R.; Kruer, W.; Schmitt, A.; Williams, E.; Stone, G. First measurement of short length-scale density fluctuations in a large laser plasma. *Phys. Rev. Lett.* **1999**, *83*, 1783. [CrossRef]
57. Toroker, Z.; Malkin, V.; Fisch, N. Seed laser chirping for enhanced backward Raman amplification in plasmas. *Phys. Rev. Lett.* **2012**, *109*, 085003. [CrossRef]
58. Malkin, V.; Shvets, G.; Fisch, N. Detuned Raman amplification of short laser pulses in plasma. *Phys. Rev. Lett.* **2000**, *84*, 1208. [CrossRef]
59. Trines, R.; Fiuza, F.; Bingham, R.; Fonseca, R.; Silva, L.; Cairns, R.; Norreys, P. Simulations of efficient Raman amplification into the multipetawatt regime. *Nat. Phys.* **2011**, *7*, 87–92. [CrossRef]
60. Ping, Y.; Cheng, W.; Suckewer, S.; Clark, D.S.; Fisch, N.J. Amplification of ultrashort laser pulses by a resonant Raman scheme in a gas-jet plasma. *Phys. Rev. Lett.* **2004**, *92*, 175007. [CrossRef]
61. Lancia, L.; Marquès, J.R.; Nakatsutsumi, M.; Riconda, C.; Weber, S.; Hüller, S.; Mančić, A.; Antici, P.; Tikhonchuk, V.; Héron, A.; et al. Experimental evidence of short light pulse amplification using strong-coupling stimulated Brillouin scattering in the pump depletion regime. *Phys. Rev. Lett.* **2010**, *104*, 025001. [CrossRef]
62. Ping, Y.; Kirkwood, R.; Wang, T.L.; Clark, D.; Wilks, S.; Meezan, N.; Berger, R.; Wurtele, J.; Fisch, N.; Malkin, V.; et al. Development of a nanosecond-laser-pumped Raman amplifier for short laser pulses in plasma. *Phys. Plasmas* **2009**, *16*, 123113. [CrossRef]
63. Ren, J.; Cheng, W.; Li, S.; Suckewer, S. A new method for generating ultraintense and ultrashort laser pulses. *Nat. Phys.* **2007**, *3*, 732–736. [CrossRef]
64. Lehmann, G.; Spatschek, K.; Sewell, G. Pulse shaping during Raman-seed amplification for short laser pulses. *Phys. Rev. E* **2013**, *87*, 063107. [CrossRef]
65. Trines, R.M.; Alves, E.; Webb, E.; Vieira, J.; Fiúza, F.; Fonseca, R.; Silva, L.; Cairns, R.A.; Bingham, R. New criteria for efficient Raman and Brillouin amplification of laser beams in plasma. *Sci. Rep.* **2020**, *10*, 19875. [CrossRef] [PubMed]
66. Lehmann, G.; Spatschek, K. Nonlinear Brillouin amplification of finite-duration seeds in the strong coupling regime. *Phys. Plasmas* **2013**, *20*, 073112. [CrossRef]
67. Sadler, J.D.; Trines, R.M.; Tabak, M.; Haberberger, D.; Froula, D.H.; Davies, A.S.; Bucht, S.; Silva, L.O.; Alves, E.P.; Fiúza, F.; et al. Optimization of plasma amplifiers. *Phys. Rev. E* **2017**, *95*, 053211. [CrossRef] [PubMed]
68. Lehmann, G.; Spatschek, K. Non-filamentated ultra-intense and ultra-short pulse fronts in three-dimensional Raman seed amplification. *Phys. Plasmas* **2014**, *21*, 053101. [CrossRef]
69. Chiaramello, M.; Amiranoff, F.; Riconda, C.; Weber, S. Role of frequency chirp and energy flow directionality in the strong coupling regime of Brillouin-based plasma amplification. *Phys. Rev. Lett.* **2016**, *117*, 235003. [CrossRef]
70. Edwards, M.R.; Mikhailova, J.M.; Fisch, N.J. X-ray amplification by stimulated Brillouin scattering. *Phys. Rev. E* **2017**, *96*, 023209. [CrossRef]
71. Sadler, J.D.; Nathvani, R.; Oleśkiewicz, P.; Ceurvorst, L.A.; Ratan, N.; Kasim, M.F.; Trines, R.M.; Bingham, R.; Norreys, P.A. Compression of X-ray free electron laser pulses to attosecond duration. *Sci. Rep.* **2015**, *5*, 16755. [CrossRef]
72. Lehmann, G.; Spatschek, K. Control of Brillouin short-pulse seed amplification by chirping the pump pulse. *Phys. Plasmas* **2015**, *22*, 043105. [CrossRef]
73. Schluck, F.; Lehmann, G.; Spatschek, K. Parametric pulse amplification by acoustic quasimodes in electron-positron plasma. *Phys. Rev. E* **2017**, *96*, 053204. [CrossRef] [PubMed]

74. Qu, K.; Barth, I.; Fisch, N.J. Plasma wave seed for Raman amplifiers. *Phys. Rev. Lett.* **2017**, *118*, 164801. [CrossRef]
75. Moody, J.; Michel, P.; Divol, L.; Berger, R.; Bond, E.; Bradley, D.; Callahan, D.; Dewald, E.; Dixit, S.; Edwards, M.; et al. Multistep redirection by cross-beam power transfer of ultrahigh-power lasers in a plasma. *Nat. Phys.* **2012**, *8*, 344–349. [CrossRef]
76. Kruer, W.L.; Wilks, S.C.; Afeyan, B.B.; Kirkwood, R.K. Energy transfer between crossing laser beams. *Phys. Plasmas* **1996**, *3*, 382–385. [CrossRef]
77. Hinkel, D.; Rosen, M.; Williams, E.; Langdon, A.; Still, C.; Callahan, D.; Moody, J.; Michel, P.; Town, R.; London, R.; et al. Stimulated Raman scatter analyses of experiments conducted at the National Ignition Facility. *Phys. Plasmas* **2011**, *18*, 056312. [CrossRef]
78. Williams, E.; Cohen, B.; Divol, L.; Dorr, M.; Hittinger, J.; Hinkel, D.; Langdon, A.; Kirkwood, R.; Froula, D.; Glenzer, S. Effects of ion trapping on crossed-laser-beam stimulated Brillouin scattering. *Phys. Plasmas* **2004**, *11*, 231–244. [CrossRef]
79. Michel, P.; Glenzer, S.; Divol, L.; Bradley, D.; Callahan, D.; Dixit, S.; Glenn, S.; Hinkel, D.; Kirkwood, R.; Kline, J.; et al. Symmetry tuning via controlled crossed-beam energy transfer on the National Ignition Facility. *Phys. Plasmas* **2010**, *17*, 056305. [CrossRef]
80. Michel, P.; Divol, L.; Williams, E.; Thomas, C.; Callahan, D.; Weber, S.; Haan, S.; Salmonson, J.; Meezan, N.; Landen, O.; et al. Energy transfer between laser beams crossing in ignition hohlraums. *Phys. Plasmas* **2009**, *16*, 042702. [CrossRef]
81. Glenzer, S.; MacGowan, B.; Michel, P.; Meezan, N.; Suter, L.; Dixit, S.; Kline, J.; Kyrala, G.; Bradley, D.; Callahan, D.; et al. Symmetric inertial confinement fusion implosions at ultra-high laser energies. *Science* **2010**, *327*, 1228–1231. [CrossRef]
82. Tanaka, K.; Goldman, L.; Seka, W.; Richardson, M.; Soures, J.; Williams, E. Stimulated Raman scattering from UV-laser-produced plasmas. *Phys. Rev. Lett.* **1982**, *48*, 1179. [CrossRef]
83. Michel, P.; Divol, L.; Dewald, E.; Milovich, J.; Hohenberger, M.; Jones, O.; Hopkins, L.B.; Berger, R.; Kruer, W.; Moody, J. Multibeam stimulated Raman scattering in inertial confinement fusion conditions. *Phys. Rev. Lett.* **2015**, *115*, 055003. [CrossRef]
84. Walsh, C.; Villeneuve, D.; Baldis, H. Electron plasma-wave production by stimulated Raman scattering: Competition with stimulated Brillouin scattering. *Phys. Rev. Lett.* **1984**, *53*, 1445. [CrossRef]
85. Froula, D.; Divol, L.; Meezan, N.; Dixit, S.; Neumayer, P.; Moody, J.; Pollock, B.; Ross, J.; Suter, L.; Glenzer, S. Laser beam propagation through inertial confinement fusion hohlraum plasmas. *Phys. Plasmas* **2007**, *14*, 055705. [CrossRef]
86. Villeneuve, D.; Baldis, H.; Bernard, J. Suppression of stimulated Raman scattering by the seeding of stimulated Brillouin scattering in a laser-produced plasma. *Phys. Rev. Lett.* **1987**, *59*, 1585. [CrossRef] [PubMed]
87. Hinkel, D.; Schneider, M.; Baldis, H.; Bonanno, G.; Bower, D.; Campbell, K.; Celeste, J.; Compton, S.; Costa, R.; Dewald, E.; et al. Laser coupling to reduced-scale hohlraum targets at the Early Light Program of the National Ignition Facility. *Phys. Plasmas* **2005**, *12*, 056305. [CrossRef]
88. Baldis, H.; Villeneuve, D.; La Fontaine, B.; Enright, G.; Labaune, C.; Baton, S.; Mounaix, P.; Pesme, D.; Casanova, M.; Rozmus, W. Stimulated Brillouin scattering in picosecond time scales: Experiments and modeling. *Phys. Fluids B Plasma Phys.* **1993**, *5*, 3319–3327. [CrossRef]
89. Lindl, J.D.; Amendt, P.; Berger, R.L.; Glendinning, S.G.; Glenzer, S.H.; Haan, S.W.; Kauffman, R.L.; Landen, O.L.; Suter, L.J. The physics basis for ignition using indirect-drive targets on the National Ignition Facility. *Phys. Plasmas* **2004**, *11*, 339–491. [CrossRef]
90. Baton, S.; Rousseaux, C.; Mounaix, P.; Labaune, C.; La Fontaine, B.; Pesme, D.; Renard, N.; Gary, S.; Louis-Jacquet, M.; Baldis, H. Stimulated Brillouin scattering with a 1 ps laser pulse in a preformed underdense plasma. *Phys. Rev. E* **1994**, *49*, R3602. [CrossRef]
91. Langdon, A.; Hinkel, D. Nonlinear evolution of stimulated scatter in high-temperature plasmas. *Phys. Rev. Lett.* **2002**, *89*, 015003. [CrossRef]
92. Mori, W.; Decker, C.; Hinkel, D.; Katsouleas, T. Raman forward scattering of short-pulse high-intensity lasers. *Phys. Rev. Lett.* **1994**, *72*, 1482. [CrossRef]
93. Matsuoka, T.; McGuffey, C.; Cummings, P.; Horovitz, Y.; Dollar, F.; Chvykov, V.; Kalintchenko, G.; Rousseau, P.; Yanovsky, V.; Bulanov, S.; et al. Stimulated Raman side scattering in laser wakefield acceleration. *Phys. Rev. Lett.* **2010**, *105*, 034801. [CrossRef] [PubMed]
94. Gordon, D.; Tzeng, K.; Clayton, C.; Dangor, A.; Malka, V.; Marsh, K.; Modena, A.; Mori, W.; Muggli, P.; Najmudin, Z.; et al. Observation of electron energies beyond the linear dephasing limit from a laser-excited relativistic plasma wave. *Phys. Rev. Lett.* **1998**, *80*, 2133. [CrossRef]
95. Rousseaux, C.; Malka, G.; Miquel, J.; Amiranoff, F.; Baton, S.; Mounaix, P. Experimental validation of the linear theory of stimulated Raman scattering driven by a 500-fs laser pulse in a preformed underdense plasma. *Phys. Rev. Lett.* **1995**, *74*, 4655. [CrossRef] [PubMed]
96. Tzeng, K.C.; Mori, W. Suppression of electron ponderomotive blowout and relativistic self-focusing by the occurrence of Raman scattering and plasma heating. *Phys. Rev. Lett.* **1998**, *81*, 104. [CrossRef]
97. Krushelnick, K.; Ting, A.; Burris, H.; Fisher, A.; Manka, C.; Esarey, E. Second harmonic generation of stimulated Raman scattered light in underdense plasmas. *Phys. Rev. Lett.* **1995**, *75*, 3681. [CrossRef]
98. Jia, Q.; Barth, I.; Edwards, M.R.; Mikhailova, J.M.; Fisch, N.J. Distinguishing Raman from strongly coupled Brillouin amplification for short pulses. *Phys. Plasmas* **2016**, *23*, 053118. [CrossRef]
99. Lehmann, G.; Spatschek, K.H. Transient plasma photonic crystals for high-power lasers. *Phys. Rev. Lett.* **2016**, *116*, 225002. [CrossRef]
100. Cairns, R. Raman amplification in plasma. In *Harnessing Relativistic Plasma Waves as Novel Radiation Sources from Terahertz to X-rays and Beyond II*; SPIE: Bellingham, WA, USA, 2011 ; Volume 8075, pp. 58–67.

101. Malkin, V.; Fisch, N.J. Key plasma parameters for resonant backward Raman amplification in plasma. *Eur. Phys. J. Spec. Top.* **2014**, *223*, 1157–1167. [CrossRef]
102. Tsidulko, Y.A.; Malkin, V.M.; Fisch, N.J. Suppression of superluminous precursors in high-power backward Raman amplifiers. *Phys. Rev. Lett.* **2002**, *88*, 235004. [CrossRef]
103. Solodov, A.; Malkin, V.; Fisch, N. Random density inhomogeneities and focusability of the output pulses for plasma-based powerful backward Raman amplifiers. *Phys. Plasmas* **2003**, *10*, 2540–2544. [CrossRef]
104. Solodov, A.; Malkin, V.; Fisch, N. Pump side scattering in ultrapowerful backward Raman amplifiers. *Phys. Rev. E* **2004**, *69*, 066413. [CrossRef]
105. Malkin, V.; Tsidulko, Y.A.; Fisch, N. Stimulated Raman scattering of rapidly amplified short laser pulses. *Phys. Rev. Lett.* **2000**, *85*, 4068. [CrossRef] [PubMed]
106. Trines, R.; Fiúza, F.; Bingham, R.; Fonseca, R.; Silva, L.; Cairns, R.; Norreys, P. Production of picosecond, kilojoule, and petawatt laser pulses via raman amplification of nanosecond pulses. *Phys. Rev. Lett.* **2011**, *107*, 105002. [CrossRef] [PubMed]
107. Yampolsky, N.A.; Malkin, V.; Fisch, N. Finite-duration seeding effects in powerful backward Raman amplifiers. *Phys. Rev. E* **2004**, *69*, 036401. [CrossRef] [PubMed]
108. Malkin, V.; Toroker, Z.; Fisch, N. Laser duration and intensity limits in plasma backward Raman amplifiers. *Phys. Plasmas* **2012**, *19*, 023109. [CrossRef]
109. Malkin, V.; Fisch, N. Relic crystal-lattice effects on Raman compression of powerful X-ray pulses in plasmas. *Phys. Rev. Lett.* **2007**, *99*, 205001. [CrossRef] [PubMed]
110. Fraiman, G.M.; Yampolsky, N.A.; Malkin, V.M.; Fisch, N.J. Robustness of laser phase fronts in backward Raman amplifiers. *Phys. Plasmas* **2002**, *9*, 3617–3624. [CrossRef]
111. Clark, D.S.; Fisch, N.J. Operating regime for a backward Raman laser amplifier in preformed plasma. *Phys. Plasmas* **2003**, *10*, 3363–3370. [CrossRef]
112. Berger, R.L.; Clark, D.S.; Solodov, A.A.; Valeo, E.J.; Fisch, N.J. Inverse bremsstrahlung stabilization of noise in the generation of ultrashort intense pulses by backward Raman amplification. *Phys. Plasmas* **2004**, *11*, 1931–1937. [CrossRef]
113. Balakin, A.; Fisch, N.; Fraiman, G.; Malkin, V.; Toroker, Z. Numerical modeling of quasitransient backward Raman amplification of laser pulses in moderately undercritical plasmas with multicharged ions. *Phys. Plasmas* **2011**, *18*, 102311. [CrossRef]
114. Malkin, V.; Fisch, N.; Wurtele, J. Compression of powerful X-ray pulses to attosecond durations by stimulated Raman backscattering in plasmas. *Phys. Rev. E* **2007**, *75*, 026404. [CrossRef] [PubMed]
115. Farmer, J.; Ersfeld, B.; Jaroszynski, D. Raman amplification in plasma: Wavebreaking and heating effects. *Phys. Plasmas* **2010**, *17*, 113301. [CrossRef]
116. Malkin, V.; Fisch, N. Quasitransient regimes of backward Raman amplification of intense X-ray pulses. *Phys. Rev. E* **2009**, *80*, 046409. [CrossRef] [PubMed]
117. Malkin, V.; Fisch, N. Quasitransient backward Raman amplification of powerful laser pulses in dense plasmas with multicharged ions. *Phys. Plasmas* **2010**, *17*, 073109. [CrossRef]
118. Phillion, D.; Banner, D.; Campbell, E.; Turner, R.; Estabrook, K. Stimulated Raman scattering in large plasmas. *Phys. Fluids* **1982**, *25*, 1434–1443. [CrossRef]
119. Prince, R.C.; Frontiera, R.R.; Potma, E.O. Stimulated Raman scattering: From bulk to nano. *Chem. Rev.* **2017**, *117*, 5070–5094. [CrossRef]
120. Liu, C.; Tripathi, V. Stimulated Raman scattering in a plasma channel. *Phys. Plasmas* **1996**, *3*, 3410–3413. [CrossRef]
121. Vieux, G.; Cipiccia, S.; Grant, D.; Lemos, N.; Grant, P.; Ciocarlan, C.; Ersfeld, B.; Hur, M.; Lepipas, P.; Manahan, G.; et al. An ultra-high gain and efficient amplifier based on Raman amplification in plasma. *Sci. Rep.* **2017**, *7*, 2399. [CrossRef]
122. Bogatskaya, A.; Volkova, E.; Popov, A. Unipolar terahertz pulse formation in a nonequilibrium plasma channel formed by an ultrashort uv laser pulse. *Phys. Rev. E* **2021**, *104*, 025202. [CrossRef]
123. Cheng, W.; Avitzour, Y.; Ping, Y.; Suckewer, S.; Fisch, N.J.; Hur, M.S.; Wurtele, J.S. Reaching the nonlinear regime of Raman amplification of ultrashort laser pulses. *Phys. Rev. Lett.* **2005**, *94*, 045003. [CrossRef]
124. Vieira, J.; Trines, R.M.; Alves, E.P.; Fonseca, R.; Mendonça, J.; Bingham, R.; Norreys, P.; Silva, L. Amplification and generation of ultra-intense twisted laser pulses via stimulated Raman scattering. *Nat. Commun.* **2016**, *7*, 10371. [CrossRef] [PubMed]
125. Chapman, T.; Hüller, S.; Masson-Laborde, P.; Heron, A.; Pesme, D.; Rozmus, W. Driven spatially autoresonant stimulated Raman scattering in the kinetic regime. *Phys. Rev. Lett.* **2012**, *108*, 145003. [CrossRef] [PubMed]
126. Edwards, M.R.; Toroker, Z.; Mikhailova, J.M.; Fisch, N.J. The efficiency of Raman amplification in the wavebreaking regime. *Phys. Plasmas* **2015**, *22*, 074501. [CrossRef]
127. Obenschain, S.; Pawley, C.; Mostovych, A.; Stamper, J.; Gardner, J.; Schmitt, A.; Bodner, S. Reduction of Raman scattering in a plasma to convective levels using induced spatial incoherence. *Phys. Rev. Lett.* **1989**, *62*, 768. [CrossRef]
128. Marchand, R.; Capjack, C.; James, C. Stimulated scattering and self-modulation of an intense laser beam in a plasma waveguide. *J. Phys. D Appl. Phys.* **1985**, *18*, 795. [CrossRef]
129. Farmer, J.; Ersfeld, B.; Jaroszynski, D. Raman Amplification in Plasma: Influence of Heating. In Proceedings of the 37th EPS Conference on Plasma Physics, Helix Arts Centre, Dublin City University Campus, Dublin, Ireland, 21–25 June 2010 ; Volume 1, p. O4.416.

130. Sharma, A.; Kourakis, I. Laser pulse compression and amplification via Raman backscattering in plasma. *Laser Part. Beams* **2009**, *27*, 579–585. [CrossRef]
131. Clark, D.; Fisch, N. Raman laser amplification in preformed and ionizing plasmas. *Laser Part. Beams* **2005**, *23*, 101–106. [CrossRef]
132. Coffey, T. Breaking of large amplitude plasma oscillations. *Phys. Fluids* **1971**, *14*, 1402–1406. [CrossRef]
133. Kim, J.; Lee, H.J.; Suk, H.; Ko, I.S. Characteristics of pulse compression in laser pulse amplification by stimulated Raman backscattering. *Phys. Lett. A* **2003**, *314*, 464–471. [CrossRef]
134. Büchner, J. Vlasov-code simulation. In Proceedings of the ISSS, Cancun, Mexico, 1–5 July 2005 ; Volume 7, pp. 26–31.
135. Atzeni, S.; Meyer-ter Vehn, J. *The Physics of Inertial Fusion: Beam Plasma Interaction, Hydrodynamics, Hot Dense Matter*; OUP Oxford: Oxford, UK, 2004; Volume 125.
136. Schiavi, A. *Study of Laser Produced Plasmas by X-ray and Proton Radiography*; Imperial College of Science, University of London: London, UK, 2003.
137. Vieux, G.; Lyachev, A.; Yang, X.; Ersfeld, B.; Farmer, J.P.; Brunetti, E.; Issac, R.; Raj, G.; Welsh, G.H.; Wiggins, S.; et al. Chirped pulse Raman amplification in plasma. *New J. Phys.* **2011**, *13*, 063042. [CrossRef]
138. Jia, Q.; Qu, K.; Fisch, N.J. Optical phase conjugation in backward Raman amplification. *Opt. Lett.* **2020**, *45*, 5254–5257. [CrossRef] [PubMed]
139. Balakin, A.; Fraiman, G.; Fisch, N.; Malkin, V. Noise suppression and enhanced focusability in plasma Raman amplifier with multi-frequency pump. *Phys. Plasmas* **2003**, *10*, 4856–4864. [CrossRef]
140. Farmer, J.P.; Pukhov, A. Raman amplification in the coherent wave-breaking regime. *Phys. Rev. E* **2015**, *92*, 063109. [CrossRef]
141. Pai, C.H.; Lin, M.W.; Ha, L.C.; Huang, S.T.; Tsou, Y.C.; Chu, H.H.; Lin, J.Y.; Wang, J.; Chen, S.Y. Backward Raman amplification in a plasma waveguide. *Phys. Rev. Lett.* **2008**, *101*, 065005. [CrossRef] [PubMed]
142. Sadler, J.D.; Silva, L.O.; Fonseca, R.A.; Glize, K.; Kasim, M.F.; Savin, A.; Aboushelbaya, R.; Mayr, M.W.; Spiers, B.; Wang, R.H.; et al. Advantages to a diverging Raman amplifier. *Commun. Phys.* **2018**, *1*, 19. [CrossRef]
143. Trines, R.M.; Fiuza, F.; Fonseca, R.A.; Silva, L.O.; Bingham, R.; Cairns, R.A.; Norreys, P.A. Numerical simulation of plasma-based Raman amplification of laser pulses to Petawatt powers. *IEEE Trans. Plasma Sci.* **2011**, *39*, 2622–2623. [CrossRef]
144. Moore, C.; Ting, A.; Krushelnick, K.; Esarey, E.; Hubbard, R.; Hafizi, B.; Burris, H.; Manka, C.; Sprangle, P. Electron trapping in self-modulated laser wakefields by Raman backscatter. *Phys. Rev. Lett.* **1997**, *79*, 3909. [CrossRef]
145. Sadler, J.D.; Sliwa, M.; Miller, T.; Kasim, M.F.; Ratan, N.; Ceurvorst, L.; Savin, A.; Aboushelbaya, R.; Norreys, P.A.; Haberberger, D.; et al. Robustness of raman plasma amplifiers and their potential for attosecond pulse generation. *High Energy Density Phys.* **2017**, *23*, 212–216. [CrossRef]
146. Ping, Y.; Geltner, I.; Fisch, N.; Shvets, G.; Suckewer, S. Demonstration of ultrashort laser pulse amplification in plasmas by a counter-propagating pumping beam. *Phys. Rev. E* **2000**, *62*, R4532. [CrossRef]
147. Ping, Y.; Geltner, I.; Morozov, A.; Fisch, N.; Suckewer, S. Raman amplification of ultrashort laser pulses in microcapillary plasmas. *Phys. Rev. E* **2002**, *66*, 046401. [CrossRef]
148. Ping, Y.; Geltner, I.; Suckewer, S. Raman backscattering and amplification in a gas jet plasma. *Phys. Rev. E* **2003**, *67*, 016401. [CrossRef] [PubMed]
149. Dreher, M.; Takahashi, E.; Meyer-ter Vehn, J.; Witte, K.J. Observation of superradiant amplification of ultrashort laser pulses in a plasma. *Phys. Rev. Lett.* **2004**, *93*, 095001. [CrossRef] [PubMed]
150. Balakin, A.A.; Kartashov, D.V.; Kiselev, A.M.; Skobelev, S.A.; Stepanov, A.N.; Fraiman, G.M. Laser pulse amplification upon Raman backscattering in plasma produced in dielectric capillaries. *J. Exp. Theor. Phys. Lett.* **2004**, *80*, 12–16. [CrossRef]
151. Shvets, G.; Fisch, N.; Pukhov, A.; Meyer-ter Vehn, J. Superradiant amplification of an ultrashort laser pulse in a plasma by a counter-propagating pump. *Phys. Rev. Lett.* **1998**, *81*, 4879. [CrossRef]
152. Fisch, N.; Malkin, V. Generation of ultrahigh intensity laser pulses. *Phys. Plasmas* **2003**, *10*, 2056–2063. [CrossRef]
153. Grech, M.; Riazuelo, G.; Pesme, D.; Weber, S.; Tikhonchuk, V. Coherent forward stimulated-brillouin scattering of a spatially incoherent laser beam in a plasma and its effect on beam spray. *Phys. Rev. Lett.* **2009**, *102*, 155001. [CrossRef] [PubMed]
154. Kirkwood, R.; Montgomery, D.; Afeyan, B.; Moody, J.; MacGowan, B.; Joshi, C.; Wharton, K.; Glenzer, S.; Williams, E.; Young, P.; et al. Observation of the nonlinear saturation of Langmuir waves driven by ponderomotive force in a large scale plasma. *Phys. Rev. Lett.* **1999**, *83*, 2965. [CrossRef]
155. Turnbull, D.; Li, S.; Morozov, A.; Suckewer, S. Simultaneous stimulated Raman, Brillouin, and electron-acoustic scattering reveals a potential saturation mechanism in Raman plasma amplifiers. *Phys. Plasmas* **2012**, *19*, 083109. [CrossRef]
156. Yang, X.; Vieux, G.; Brunetti, E.; Ersfeld, B.; Farmer, J.P.; Hur, M.S.; Issac, R.; Raj, G.; Wiggins, S.; Welsh, G.; et al. Chirped pulse Raman amplification in warm plasma: Towards controlling saturation. *Sci. Rep.* **2015**, *5*, 13333. [CrossRef]
157. Bullock, A.B.; Bolton, P.R.; Mayer, F.J. Time-integrated reflectivity of laser-induced back-ablated aluminum thin film targets. *J. Appl. Phys.* **1997**, *82*, 1828–1831. [CrossRef]
158. Perkins, F.; Oberman, C.; Valeo, E. Parametric instabilities and ionospheric modification. *J. Geophys. Res.* **1974**, *79*, 1478–1496. [CrossRef]
159. Kirkwood, R.; Dewald, E.; Niemann, C.; Meezan, N.; Wilks, S.; Price, D.; Landen, O.; Wurtele, J.; Charman, A.; Lindberg, R.; et al. Amplification of an ultrashort pulse laser by stimulated Raman scattering of a 1 ns pulse in a low density plasma. *Phys. Plasmas* **2007**, *14*, 113109. [CrossRef]

160. Chiaramello, M. Laser Amplification via Stimulated Brillouin Scattering in the Strongly Coupled Regime: Towards Control and Optimization. Ph.D. Thesis, Université Pierre et Marie Curie, Paris, France, 2016.
161. Guillaume, E.; Humphrey, K.; Nakamura, H.; Trines, R.; Heathcote, R.; Galimberti, M.; Amano, Y.; Doria, D.; Hicks, G.; Higson, E.; et al. Demonstration of laser pulse amplification by stimulated Brillouin scattering. *High Power Laser Sci. Eng.* **2014**, *2* , e33. [CrossRef]
162. Gorbunov, L. Perturbation of a medium by a field of a strong electromagnete wave. *Sov. Phys. JETP* **1969**, *28*, 1220–1225.
163. Liu, C.; Kaw, P. Parametric instabilities in homogeneous unmagnetized plasmas. *Adv. Plasma Phys.* **1976**, *6*, 83–119.
164. Zakharov, V.; Musher, S.; Rubenchik, A. Hamiltonian approach to the description of non-linear plasma phenomena. *Phys. Rep.* **1985**, *129*, 285–366. [CrossRef]
165. Liu, C.; Rosenbluth, M.N.; White, R.B. Raman and Brillouin scattering of electromagnetic waves in inhomogeneous plasmas. *Phys. Fluids* **1974**, *17*, 1211–1219. [CrossRef]
166. Schluck, F.; Lehmann, G.; Spatschek, K. Amplification of a seed pumped by a chirped laser in the strong coupling Brillouin regime. *Phys. Plasmas* **2015**, *22*, 093104. [CrossRef]
167. Andreev, A.; Riconda, C.; Tikhonchuk, V.; Weber, S. Short light pulse amplification and compression by stimulated Brillouin scattering in plasmas in the strong coupling regime. *Phys. Plasmas* **2006**, *13*, 053110. [CrossRef]
168. Edwards, M.R.; Jia, Q.; Mikhailova, J.M.; Fisch, N.J. Short-pulse amplification by strongly coupled stimulated Brillouin scattering. *Phys. Plasmas* **2016**, *23*, 083122. [CrossRef]
169. Li, Z.; Zuo, Y.; Su, J.; Yang, S. The filamentation effect in short pulse amplification by strong-coupling stimulated Brillouin scattering. *Phys. Plasmas* **2019**, *26*, 093102. [CrossRef]
170. Alves, P.; Trines, R.; Humphrey, K.; Bingham, R.; Cairns, A.; Fiuza, F.; Fonseca, R.; Silva, L.; Norreys, P. A robust plasma-based laser amplifier via stimulated Brillouin scattering. *arXiv* **2013**, arXiv:1311.2034v3.
171. Clark, D.S.; Fisch, N.J. Particle-in-cell simulations of Raman laser amplification in preformed plasmas. *Phys. Plasmas* **2003**, *10*, 4848–4855. [CrossRef]
172. Humphrey, K.; Trines, R.; Fiuza, F.; Speirs, D.; Norreys, P.; Cairns, R.; Silva, L.; Bingham, R. Effect of collisions on amplification of laser beams by Brillouin scattering in plasmas. *Phys. Plasmas* **2013**, *20*, 102114. [CrossRef]
173. Trines, R.; Alves, E.; Humphrey, K.; Bingham, R.; Cairns, R.; Fiuza, F.; Fonseca, R.; Silva, L.; Norreys, P. Boosting the performance of Brillouin amplification at sub-quarter-critical densities via reduction of parasitic Raman scattering. *arXiv* **2014**, arXiv:1406.5424.
174. Gibbon, P. *Short Pulse Laser Interactions with Matter: An Introduction*; Imperial College Press: London, UK; World Scientific Publishing Co. Pte. Ltd.: Singapore, 2005.
175. Kruer, W. *The Physics of Laser Plasma Interactions*; CRC Press, Taylor & Francis Group: Boca Raton, FL, USA, 2019.
176. Kaw, P.; Schmidt, G.; Wilcox, T. Filamentation and trapping of electromagnetic radiation in plasmas. *Phys. Fluids* **1973**, *16*, 1522–1525. [CrossRef]
177. Max, C.E.; Arons, J.; Langdon, A.B. Self-modulation and self-focusing of electromagnetic waves in plasmas. *Phys. Rev. Lett.* **1974**, *33*, 209. [CrossRef]
178. Ting, A.; Moore, C.; Krushelnick, K.; Manka, C.; Esarey, E.; Sprangle, P.; Hubbard, R.; Burris, H.; Fischer, R.; Baine, M. Plasma wakefield generation and electron acceleration in a self-modulated laser wakefield accelerator experiment. *Phys. Plasmas* **1997**, *4*, 1889–1899. [CrossRef]
179. Perkins, F.; Valeo, E. Thermal self-focusing of electromagnetic waves in plasmas. *Phys. Rev. Lett.* **1974**, *32*, 1234. [CrossRef]
180. Epperlein, E.M. Kinetic theory of laser filamentation in plasmas. *Phys. Rev. Lett.* **1990**, *65*, 2145. [CrossRef]
181. Weber, S.; Riconda, C.; Lancia, L.; Marques, J.R.; Mourou, G.; Fuchs, J. Amplification of ultrashort laser pulses by Brillouin backscattering in plasmas. *Phys. Rev. Lett.* **2013**, *111*, 055004. [CrossRef]
182. Shvets, G.; Wurtele, J.; Shadwick, B. Analysis and simulation of Raman backscatter in underdense plasmas. *Phys. Plasmas* **1997**, *4*, 1872–1880. [CrossRef]
183. Nuter, R.; Tikhonchuk, V. Prepulse suppression and optimization of backward Raman amplification with a chirped pump laser beam. *Phys. Rev. E* **2013**, *87*, 043109. [CrossRef]
184. Vieux, G.; Ersfeld, B.; Farmer, J.P.; Hur, M.S.; Issac, R.; Jaroszynski, D. Plasma density measurements using chirped pulse broad-band Raman amplification. *Appl. Phys. Lett.* **2013**, *103*, 121106. [CrossRef]
185. Ersfeld, B.; Jaroszynski, D. Superradiant linear Raman amplification in plasma using a chirped pump pulse. *Phys. Rev. Lett.* **2005**, *95*, 165002. [CrossRef] [PubMed]
186. Chiaramello, M.; Riconda, C.; Amiranoff, F.; Fuchs, J.; Grech, M.; Lancia, L.; Marquès, J.R.; Vinci, T.; Weber, S. Optimization of interaction conditions for efficient short laser pulse amplification by stimulated Brillouin scattering in the strongly coupled regime. *Phys. Plasmas* **2016**, *23*, 072103. [CrossRef]
187. Riconda, C.; Weber, S.; Lancia, L.; Marquès, J.R.; Mourou, G.; Fuchs, J. Spectral characteristics of ultra-short laser pulses in plasma amplifiers. *Phys. Plasmas* **2013**, *20*, 083115. [CrossRef]
188. Edwards, M.R.; Shi, Y.; Mikhailova, J.M.; Fisch, N.J. Laser amplification in strongly magnetized plasma. *Phys. Rev. Lett.* **2019**, *123*, 025001. [CrossRef]
189. Li, Z.; Wu, Z.; Zuo, Y.; Zeng, X.; Wang, X.; Wang, X.; Mu, J.; Hu, B.; Su, J. Boosting strong-coupling stimulated Brillouin amplification performance using an external magnetic field. *Phys. Plasmas* **2021**, *28*, 013107. [CrossRef]

190. Trines, R.; Alves, E.; Webb, E.; Vieira, J.; Fiuza, F.; Fonseca, R.; Silva, L.; Sadler, J.; Ratan, N.; Ceurvorst, L.; et al. Essential criteria for efficient pulse amplification via Raman and Brillouin scattering. *arXiv* **2016**, arXiv:1611.04485.
191. Trines, R.M.; Alves, E.P.; Humphrey, K.; Bingham, R.; Cairns, R.A.; Fiúza, F.; Fonseca, R.; Silva, L.O. Boosting the performance of Brillouin amplification at sub-quarter-critical densities via reduction of parasitic Raman scattering. *Plasma Phys. Control. Fusion* **2021**, *63*, 124003. [CrossRef]
192. Krupke, W. Rare earth vapor laser studies. In Proceedings of the 13th Rare Earth Research Conference, Olgebay Park, WV, USA, 16 October 1977.
193. Yablonovitch, E.; Goldhar, J. Short CO_2 laser pulse generation by optical free induction decay. *Appl. Phys. Lett.* **1974**, *25*, 580–582. [CrossRef]
194. Fisher, R.A.; Feldman, B. Generation of single ultrashort CO_2 laser pulses in a Fabry–Perot interferometer. *Opt. Lett.* **1977**, *1*, 161–163. [CrossRef] [PubMed]
195. Cohen, B.I.; Kaufman, A.N. Effects of beat-wave electron trapping on stimulated Raman and Thomson scattering. *Phys. Fluids* **1978**, *21*, 404–412. [CrossRef]
196. Zhang, Z.; Zhang, B.; Hong, W.; Deng, Z.; Teng, J.; He, S.; Zhou, W.; Gu, Y. Generation of high-power few-cycle lasers via Brillouin-based plasma amplification. *Phys. Plasmas* **2017**, *24*, 113104. [CrossRef]
197. Turnbull, D.; Bucht, S.; Davies, A.; Haberberger, D.; Kessler, T.; Shaw, J.; Froula, D. Raman amplification with a flying focus. *Phys. Rev. Lett.* **2018**, *120*, 024801. [CrossRef]
198. Afeyan, B.; Hüller, S. Optimal control of laser plasma instabilities using Spike Trains of Uneven Duration and Delay (STUD pulses) for ICF and IFE. In *EPJ Web of Conferences* ; EDP Sciences: Les Ulis, France, 2013; Volume 59, p. 05009.
199. Lehmberg, R.; Obenschain, S. Use of induced spatial incoherence for uniform illumination of laser fusion targets. *Opt. Commun.* **1983**, *46*, 27–31. [CrossRef]
200. Mostovych, A.; Obenschain, S.; Gardner, J.; Grun, J.; Kearney, K.; Manka, C.; McLean, E.; Pawley, C. Brillouin scattering measurements from plasmas irradiated with spatially and temporally incoherent laser light. *Phys. Rev. Lett.* **1987**, *59*, 1193. [CrossRef]
201. Shoucri, M.; Matte, J.P.; Vidal, F. Relativistic Eulerian Vlasov simulations of the amplification of seed pulses by Brillouin backscattering in plasmas. *Phys. Plasmas* **2015**, *22*, 053101. [CrossRef]
202. Lehmann, G.; Spatschek, K. Temperature dependence of seed pulse amplitude and density grating in Brillouin amplification. *Phys. Plasmas* **2016**, *23*, 023107. [CrossRef]
203. Humphrey, K.; Trines, R.; Alves, E.; Fiúza, F.; Speirs, D.; Bingham, R.; Cairns, R.; Fonseca, R.; Silva, L.; Norreys, P. Production of petawatt laser pulses of picosecond duration via Brillouin amplification of nanosecond laser beams. *arXiv* **2013**, arXiv:1311.2034v1.
204. Kirkwood, R.; Michel, P.; London, R.; Moody, J.; Dewald, E.; Yin, L.; Kline, J.; Hinkel, D.; Callahan, D.; Meezan, N.; et al. Multi-beam effects on backscatter and its saturation in experiments with conditions relevant to ignition. *Phys. Plasmas* **2011**, *18*, 056311. [CrossRef]
205. Edwards, M.R.; Fisch, N.J.; Mikhailova, J.M. Strongly enhanced stimulated Brillouin backscattering in an electron-positron plasma. *Phys. Rev. Lett.* **2016**, *116*, 015004. [CrossRef]
206. Guo, Q.; Lu, Z.; Wang, Y. Highly efficient Brillouin amplification of strong Stokes seed. *Appl. Phys. Lett.* **2010**, *96*, 221107. [CrossRef]
207. Bel'dyugin, I.; Efimkov, V.; Mikhailov, S.; Zubarev, I. Amplification of weak Stokes signals in the transient regime of stimulated Brillouin scattering. *J. Russ. Laser Res.* **2005**, *26*, 1–12. [CrossRef]
208. Lu, Z.; Gao, W.; He, W.; Zhang, Z.; Hasi, W. High amplification and low noise achieved by a double-stage non-collinear Brillouin amplifier. *Opt. Express* **2009**, *17*, 10675–10680. [CrossRef]
209. Sternklar, S.; Jackel, S.; Chomsky, D.; Zigler, A. Coherent beam and image amplification by Brillouin two-beam coupling in CS 2. *Opt. Lett.* **1990**, *15*, 616–618. [CrossRef]
210. Yin, L.; Albright, B.; Rose, H.; Bowers, K.; Bergen, B.; Kirkwood, R.; Hinkel, D.; Langdon, A.; Michel, P.; Montgomery, D.; et al. Trapping induced nonlinear behavior of backward stimulated Raman scattering in multi-speckled laser beams. *Phys. Plasmas* **2012**, *19*, 056304. [CrossRef]
211. Kirkwood, R.; MacGowan, B.; Montgomery, D.; Afeyan, B.; Kruer, W.; Moody, J.; Estabrook, K.; Back, C.; Glenzer, S.; Blain, M.; et al. Effect of ion-wave damping on stimulated Raman scattering in high-Z laser-produced plasmas. *Phys. Rev. Lett.* **1996**, *77*, 2706. [CrossRef]
212. Ren, J.; Li, S.; Morozov, A.; Suckewer, S.; Yampolsky, N.; Malkin, V.; Fisch, N. A compact double-pass Raman backscattering amplifier/compressor. *Phys. Plasmas* **2008**, *15*, 056702. [CrossRef]
213. Mishra, S.; Andreev, A. Amplification of ultra-short laser pulses via resonant backward Raman amplification in plasma. *Phys. Plasmas* **2016**, *23*, 083108. [CrossRef]
214. Mardahl, P.; Lee, H.J.; Penn, G.; Wurtele, J.; Fisch, N. Intense laser pulse amplification using Raman backscatter in plasma channels. *Phys. Lett. A* **2002**, *296*, 109–116. [CrossRef]
215. Yampolsky, N.; Fisch, N.; Malkin, V.; Valeo, E.; Lindberg, R.; Wurtele, J.; Ren, J.; Li, S.; Morozov, A.; Suckewer, S. Demonstration of detuning and wavebreaking effects on Raman amplification efficiency in plasma. *Phys. Plasmas* **2008**, *15*, 113104. [CrossRef]
216. Turnbull, D.; Li, S.; Morozov, A.; Suckewer, S. Possible origins of a time-resolved frequency shift in Raman plasma amplifiers. *Phys. Plasmas* **2012**, *19*, 073103. [CrossRef]

217. Depierreux, S.; Yahia, V.; Goyon, C.; Loisel, G.; Masson-Laborde, P.E.; Borisenko, N.; Orekhov, A.; Rosmej, O.; Rienecker, T.; Labaune, C. Laser light triggers increased Raman amplification in the regime of nonlinear Landau damping. *Nat. Commun.* **2014**, *5*, 4158. [CrossRef] [PubMed]
218. Toroker, Z.; Malkin, V.; Fisch, N. Backward Raman amplification in the Langmuir wavebreaking regime. *Phys. Plasmas* **2014**, *21*, 113110. [CrossRef]
219. Edwards, M.R.; Qu, K.; Mikhailova, J.M.; Fisch, N.J. Beam cleaning of an incoherent laser via plasma Raman amplification. *Phys. Plasmas* **2017**, *24*, 103110. [CrossRef]
220. Lehmann, G.; Schluck, F.; Spatschek, K. Regions for Brillouin seed pulse growth in relativistic laser-plasma interaction. *Phys. Plasmas* **2012**, *19*, 093120. [CrossRef]
221. Jia, Q.; Shi, Y.; Qin, H.; Fisch, N.J. Kinetic simulations of laser parametric amplification in magnetized plasmas. *Phys. Plasmas* **2017**, *24*, 093103. [CrossRef]
222. Matsuo, K.; Nagatomo, H.; Zhang, Z.; Nicolai, P.; Sano, T.; Sakata, S.; Kojima, S.; Lee, S.H.; Law, K.F.F.; Arikawa, Y.; et al. Magnetohydrodynamics of laser-produced high-energy-density plasma in a strong external magnetic field. *Phys. Rev. E* **2017**, *95*, 053204. [CrossRef]
223. Stix, T.H. *Waves in Plasmas*; Springer: New York, NY, USA, 1992 .
224. Sprangle, P.; Esarey, E.; Ting, A. Nonlinear theory of intense laser-plasma interactions. *Phys. Rev. Lett.* **1990**, *64*, 2011. [CrossRef] [PubMed]
225. Laqua, H.P. Electron Bernstein wave heating and diagnostic. *Plasma Phys. Control. Fusion* **2007**, *49*, R1. [CrossRef]
226. Shi, Y.; Qin, H.; Fisch, N.J. Laser-pulse compression using magnetized plasmas. *Phys. Rev. E* **2017**, *95*, 023211. [CrossRef] [PubMed]
227. Arber, T.; Bennett, K.; Brady, C.; Lawrence-Douglas, A.; Ramsay, M.; Sircombe, N.; Gillies, P.; Evans, R.; Schmitz, H.; Bell, A.; et al. Contemporary particle-in-cell approach to laser-plasma modelling. *Plasma Phys. Control. Fusion* **2015**, *57*, 113001. [CrossRef]
228. Shi, Y.; Fisch, N.J. Amplification of mid-infrared lasers via magnetized-plasma coupling. *arXiv* **2019**, arXiv:1904.05536.
229. Shi, Y.; Qin, H.; Fisch, N.J. Laser-plasma interactions in magnetized environment. *Phys. Plasmas* **2018**, *25*, 055706. [CrossRef]